Top Curr Chem (2009) 288: 67–107
DOI: 10.1007/128_2008_13

Published online: 13 March 2009

Structure, Function, and Assembly of Type 1 Fimbriae

Stefan D. Knight and Julie Bouckaert

Abstract Bacterial infections constitute a major global health problem, acutely accentuated by the rapid spread of antibiotic resistant bacterial strains. The widespread need for bacteria to attach – adhere – to target cells before they can initiate an infection may be used to advantage by targeting the bacterial adhesion tools such as pili and fimbriae for development of novel anti-bacterial vaccines and drugs. Type 1 fimbriae are widely expressed by *Escherichia coli* and are used by uropathogenic strains to mediate attachment to specific niches in the urinary tract. These fimbriae belong to a class of fibrillar adhesion organelles assembled through the chaperone/usher pathway, one of the terminal branches of the general secretion pathway in Gram-negative bacteria. Our understanding of the assembly, structure and function of these structures has evolved significantly over the last decade. Here, we summarize current understanding of the function and biogenesis of fibrillar adhesion organelles, and provide some examples of recent progress towards interfering with bacterial adhesion as a means to prevent infection.

Keywords Assembly, Bacterial adhesion, Chaperone/Usher pathway, Fimbriae/Pili, Lectin

Contents

1 Introduction 68
2 SDA and TDA Fimbrial Adhesins: Ultrastructure and Assembly 68
2.1 Fibre Structure 70
2.2 Fibre Biogenesis 72

S.D. Knight (✉)
Swedish University of Agricultural Sciences, Department of Molecular Biology,
Uppsala Biomedical Center, PO Box 590, 75124 Uppsala, Sweden
e-mail: stefan.knight@molbio.slu.se

J. Bouckaert
Vrije Universiteit Brussel, Ultrastructure Laboratory, Pleinlaan 2, B1050 Brussels, Belgium
VIB, Department of Molecular and Cellular Interactions, Belgium

3 Type 1 Fimbriae 79
3.1 Genetic Organization and Regulation 80
3.2 Role in Disease and Biofilm Formation 82
3.3 Receptors in the Urinary Tract 84
3.4 The FimH Adhesin 85
3.5 Factors that Enhance Adhesion 93
3.6 Medical Applications 96
4 Conclusion and Perspectives 100
References 101

Abbreviations

C-HEGA	cyclohexylbutanoyl-*N*-hydroxyethyl glucamide
DSC	donor stand complementation
DSE	donor strand exchange
ETEC	enterotoxigenic *E. coli*
H-NS	histone-like nucleoid-structuring protein
IBC	intracellular bacterial community
Ig	immunoglobulin
IHF	integration host factor
IM	inner membrane
Lrp	leucine-responsive regulatory protein
OM	outer membrane
SAM	self-assembled monolayer
SDA	single-domain adhesin
TDA	two-domain adhesin
THP	Tamm-Horsfall protein
UPEC	uropathogenic *E. coli*
UTI	urinary tract infection

1 Introduction

Infectious diseases constitute a major global health and health cost burden. The World Health Report 2004 [1] estimates that infectious and parasitic diseases caused almost 11 million deaths in 2002. The same report estimates that respiratory and diarrhoeal infections were responsible for 4.0 and 1.8 million deaths, respectively, in 2002, to be compared to the toll of diseases such as AIDS (2.8 million deaths), tuberculosis (1.6 million deaths), and malaria (1.3 million deaths). A significant proportion of respiratory and diarrhoeal infections are caused by Gram-negative pathogens such as *Salmonella enterica* (typhoid fever, enterocolitis), *Haemophilus influenzae* (pneumonia), *Bordetella pertussis* (whooping cough), and *Escherichia coli* (diarrhoea). The overwhelming majority of the world's annual 4 million neonatal deaths occur in developing countries. Bacterial infection is the major cause of neonatal admissions to hospitals, and probably the

biggest cause of morbidity in the community. The most common serious neonatal infections involve bacteraemia, meningitis, and respiratory tract infections, and case fatality rates may be as high as 45%. Key pathogens in these infections are *E. coli*, *Klebsiella* sp., *Staphylococcus aureus* and *Streptococcus pyogenes* [2].

Although it remains true that bacterial infections can often be efficiently treated with antibiotics, the emergence of antibiotic resistant bacterial strains is a serious problem [3, 4]. For example, treatment of typhoid fever relies on prompt administration of antibiotics, but strains of *S. typhi* resistant to one or more of the commonly used antibiotics have emerged worldwide [5]. *E. coli* infections in humans (mostly urinary tract infections (UTIs)) can normally be treated with antibiotics, but again, the emergence of antibiotic resistant bacterial strains poses a serious and growing threat [6–8]. In light of this, the use of antibiotics in the treatment and control of human as well as of animal infections should be minimized, and development of novel strategies to treat and prevent bacterial infections are urgently needed [3].

One aspect of the pathogen-host interaction that shows great promise as a target for development of novel means of interfering with bacterial infections is the early establishment of physical contact between pathogen and host. Adhesion of bacteria to target tissues is frequently a necessary first step in pathogenesis [9–11]. For example, uropathogenic *E. coli* (UPEC) depend on specific binding to mannose-containing receptors on the luminal surface of the bladder epithelium for the establishment of cystitis (bladder infection) [12–16], whereas binding to Galα1–4Gal-containing receptors in the upper urinary tract is a prerequisite for the establishment of pyelonephritis (kidney infection) [17]. Blocking of adhesion can provide an efficient way of interfering with bacterial infections. For example, blocking binding to mannose-containing receptors has been shown to prevent UPEC adhesion to the bladder uroepithelium and cystitis [13, 14, 18, 19]. Similarly, blocking the binding of UPEC to Galα1–4Gal-containing receptors can prevent adhesion to and infection of kidney epithelium [20, 21].

Most bacteria depend on expression of specialized adhesive organelles on the bacterial cell surface to mediate attachment to target tissues. Gram-negative bacteria can grow hair-like adhesive organelles referred to as pili (from the Latin word for 'hair') or fimbriae (from the Latin word for 'thread') [22] arranged in a multitude of 'hairstyles' ranging from soft, long, wavy hair, to afro style (Fig. 1). In one common class of such fibrillar organelles [25], many copies of a receptor binding 'single-domain adhesin' (SDA) are incorporated in a thin (2–5 nm wide) and flexible fibre. Examples of such 'polyadhesins' include the Dr adhesins expressed by many UPEC strains, SEF14 fimbriae of *Salmonella enteritidis*, Myf fimbriae of *Yersinia enterocolitica*, and the pH6 and F1 antigens expressed by *Yersinia pestis*. A second class of fibrillar adhesive organelle commonly expressed by Gram-negative pathogens display a carbohydrate-binding 'two-domain adhesin' (TDA) at the tip of complex pili or fimbriae. These composite structures frequently incorporate the TDA at the tip of a thin (~2 nm) and flexible 'tip fibrillum' linked to a relatively rigid 1–2 μm long and ~8 nm wide 'stalk' or 'rod', consisting of a helically wound fibre of fimbrial subunits ('pilins'). Examples of TDA-displaying adhesive organelles include the much studied P pili, and type 1 fimbriae (the main focus of this chapter) that provide UPEC with the ability to bind to Galα1–4Gal-containing and mannose-containing receptors

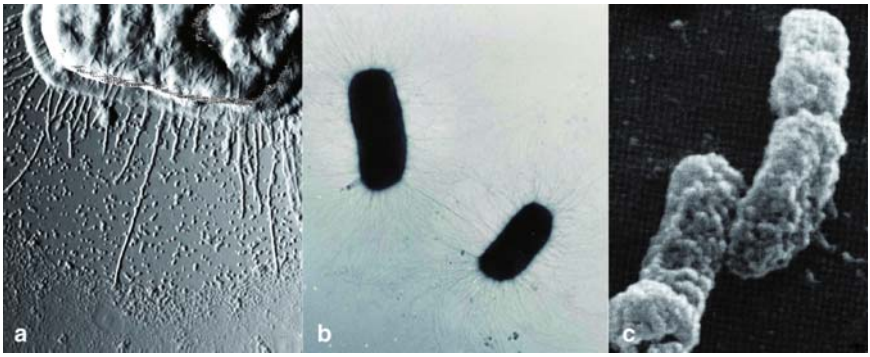

Fig. 1 Examples of bacterial 'hair styles'. **a** Thick and straight: type 1 fimbriated *E. coli*. Type 1 fimbriae are composite structures with a relatively rigid 8 nm wide rod tipped by a thin (2.5 nm) more flexible tip fibrillum. **b** Thin and wavy: F17 fimbriated *E. coli* covered with 1–3 μm long, flexible, 2–3 nm wide fimbriae. **c** Tangled (capsules and sheaths): *Y. pestis* F1 capsular antigen. No individual fibres are visible, but the capsule consists of a tangle of thin (~2 nm) flexible fibres. AFM amplitude picture (**a**) kindly provided by Dr R. Willaert, Ultrastructure, VU Brussels; TEM picture (**b**) kindly provided by I. Caplier, Protein Chemistry, VU Brussels and reprinted from [23] with permission from the publisher; SEM picture (**c**) reprinted from [24] with permission from the publisher

respectively, and that are important for UPEC colonization of the urinary tract. The specialized SDA and TDA bacterial adhesive organelles provide promising targets for development of new classes of anti-bacterial drugs that may either directly block adhesion or interfere with the biogenesis of adhesive organelles, and for the development of novel vaccines to prevent bacterial infections.

2 SDA and TDA Fimbrial Adhesins: Ultrastructure and Assembly

Results from structure-based studies of components of the P pilus, type 1 fimbriae, and F1 antigen systems over the last 8 or so years have led to a relatively refined understanding of how SDA and TDA fimbrial adhesins are constructed, and of how periplasmic chaperones direct and promote their assembly. Key to the success of these studies has been the realization that the fimbrial subunits, although very unstable on their own, can be isolated as stable complexes with their cognate periplasmic chaperone, and that assembly can be blocked by mutations in the N-terminal region of the subunits, allowing isolation and characterization of assembly intermediates. These studies have shown that, in spite of a great deal of variation in appearance and binding specificity, a large group of bacterial pili/fimbriae share the same underlying fibre structure, consisting of a string of non-covalently linked immunoglobulin (Ig)-like modules. This linear fibre structure is assembled from monomeric, incomplete Ig subunits by a periplasmic chaperone together with an outer

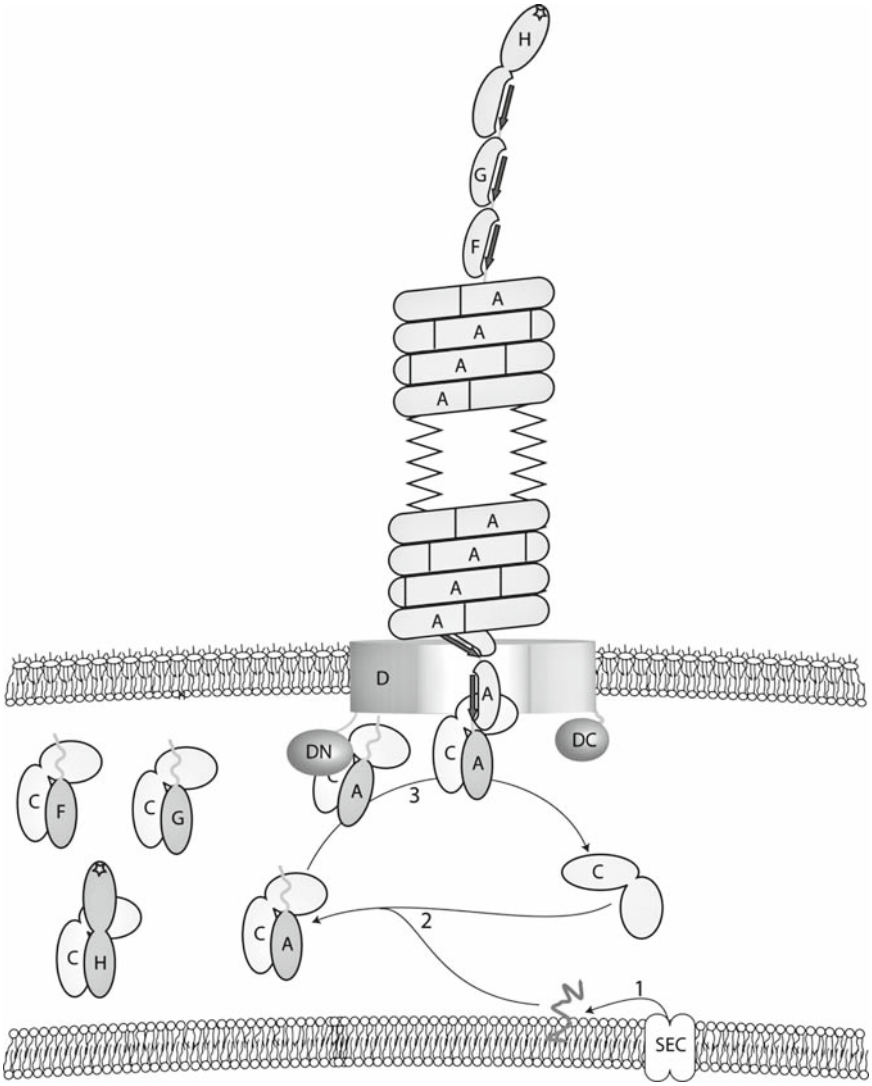

Fig. 2 Schematic illustration of chaperone/usher-assisted assembly of type 1 fimbriae. Subunits (A, F, G, H) enter the periplasm via the Sec system and transiently remain associated with the inner membrane (step 1). FimC chaperone (C) binds newly translocated, partially unfolded subunits to form soluble and stable chaperone:subunit complexes (step 2). Targeting of the binary FimC:FimH pre-assembly complex to an empty FimD usher (D) initiates assembly. At the usher, an incoming chaperone:subunit complex attacks the chaperone:subunit complex capping the base of the growing fibre (step 3). The usher catalyses DSE in which the capping chaperone at the base is released, the N-terminal G_d donor strand of the attacking subunit is inserted into the polymerization cleft of the subunit at the base to form a new fibre module, and a new chaperone-capped subunit is added at the base. For further details of the assembly process, see text

membrane usher (Fig. 2) [9, 11, 26–31]. The final fibre morphology is determined by additional interactions between non-adjacent pilin subunits in the fibre, allowing some fibres to coil into rigid helical structures such as the fimbrial rods, while some remain as relatively flexible extended linear fibres that sometimes collapse into amorphous 'sheaths' or 'capsules'. The structural pilin subunits of complex fimbriae, and the SDA subunits of polyadhesins, have the same basic architecture and are assembled in the same manner.

2.1 Fibre Structure

The subunits of fimbriae are constructed essentially as Ig-like β-sandwiches, but with a circular permutation that positions the sequence corresponding to the seventh, C-terminal, Ig β-strand (strand G of a canonical Ig domain) at the N-terminus of the polypeptide sequence [32–35] (Figs. 3a and 4a). In a typical Ig fold, the 'top' edge of the sandwich, defined by the A and F strands, is capped by the C-terminal G strand, which is hydrogen bonded to the F strand and provides hydrophobic residues to the core of the fold. Free pilin subunits are only marginally stable, and no structure for a monomeric pilin in the absence of chaperone has been obtained. Sometimes, in the absence of the chaperone, soluble, domain-swapped pilin dimers [36] or trimers [37, 38] are formed and have been reported in their crystal structures. However, the oligomerization of pilins in this manner is a dead-end process, and the pilins in these oligomers are not able to assemble into fibrillar structures.

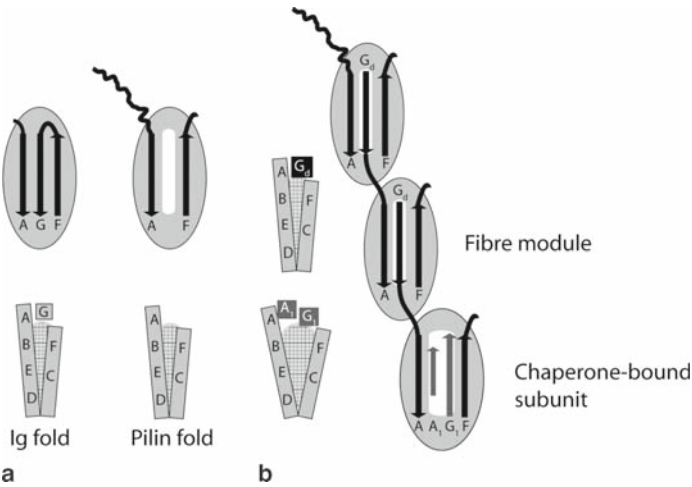

Fig. 3 Schematic illustration of: **a** relation between the Ig and the pilin fold; **b** DSC before (subunit bound to chaperone; *below*) and after (in fibre module; *above*) DSE. The ellipsoids represent the β-sandwich of the Ig/pilin fold as viewed down at the AF edge of the sandwich; the rectangles represent β sheets and strands (*as labelled*) viewed edge on

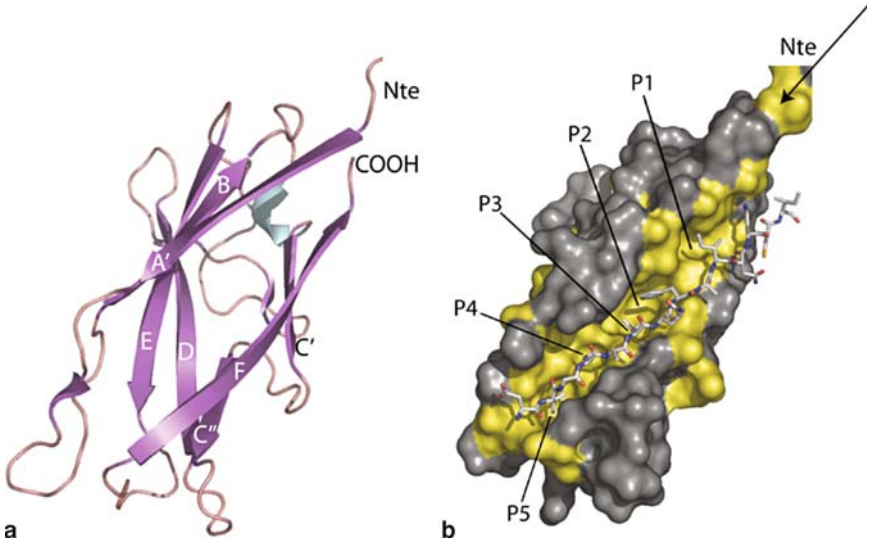

Fig. 4 Pilin structure: **a** ribbon diagram of a Caf1 subunit illustrating the Ig-like pilin fold. Main secondary structural elements are labelled; Nte denotes the N-terminal extension (disordered unless used for DSC of a neighbouring subunit in a fibre); **b** surface representation of Caf1 illustrating the hydrophobic acceptor cleft (hydrophobic residues Ala, Val, Leu, Ile, Phe, Met *coloured yellow*) with the G_d strand from the Caf1M chaperone (*stick model*) bound; sub-pockets of the acceptor cleft, designated P1-P5 in the nomenclature of Sauer et al. [34], are labelled

Various structures of pilins bound to chaperone or peptides [32–34, 39, 40], or incorporated into fibres [35, 41], show that in the absence of a seventh β-strand, a pilin subunit cannot cap its AF edge, and a closed hydrophobic core is not formed. Instead, a deep hydrophobic cleft is created on the surface of the subunit (Fig. 4b). The hydrophobic effect drives folding of globular proteins by favouring the packing of hydrophobic side chains together in a hydrophobic core, shielded from the surrounding water. In pilins, however, owing to the absence of a seventh C-terminal (G) strand, the polypeptide chain simply cannot fold in such a way as to create a shielded hydrophobic core, explaining the instability of free pilin subunits.

The N-terminal extension of pilins, which is flexible in solution and does not contribute to the subunit's globular fold, carries a β-strand motif of alternating hydrophobic and hydrophilic residues. Deletions or mutations in this N-terminal region block assembly of pilin subunits into fibres [34, 35, 39, 41–44]. The structure of a Caf1M:$(Caf1)_2$ ternary complex [35, 41], with the minimal *Y. pestis* F1-antigen fibre ($(Caf1)_2$) bound to the Caf1M chaperone, revealed that fibre subunits are linked together by insertion of the N-terminal extension of one subunit into the hydrophobic cleft of the second subunit (Fig. 3b). The inserted N-terminal segment adopts a β-strand conformation running antiparallel to the F strand, with hydrophobic side chains bound in three (TDA systems) or five (SDA systems) acceptor cleft sub-pockets (Fig. 4b), hence completing the Ig fold of the subunit. This mode of binding, termed 'donor strand complementation' (DSC), had previously been predicted for

type 1 and P pilus fibres [32–34], and is likely to be present in all surface polymers assembled through the chaperone/usher pathway. The resulting linear fibre is composed of globular modules each having an intact Ig topology generated by DSC (Fig. 3b). In this fibre, each Ig module is made from two polypeptide chains, with the G strand being provided in trans (because the N-terminal segment of one subunit is donated to fulfil the role of the Ig-fold G strand in a second subunit, the N-terminal sequence is also referred to as the G_d (d for donor) sequence). TDAs lack the N-terminal G_d polymerization sequence and instead have an entire receptor-binding domain coupled to the N-terminus of the pilin domain. As a consequence, TDAs can only be incorporated in a single copy at the tip of fimbriae. In earlier work based on immunogold labelling, the FimH adhesin was reported to be laterally located along the type 1 fimbrial shaft [45]. However this is contradicted by later findings, using quick-freeze deep-etch electron microscopy [46], or gold-coupled antibodies in combination with transmission electron microscopy [47], and is incongruent with current understanding of fimbrial structure and assembly.

In spite of their non-covalent nature, and in contrast to free pilins, or pilin subunits bound to their chaperone, studies of the *Y. pestis* F1 antigen system have shown that the fibre Ig modules can be extremely stable. The folding free energy estimated from reversible unfolding of an engineered monomeric F1 fibre module (Caf1-SC) in GdmCl at 37 °C is in the range 70–80 kJ mol^{-1} [41]. This should be compared to the typical range of 20–60 kJ mol^{-1} maximum stability for stable proteins in physiological conditions [48, 49]. This apparently narrow range of optimal stability for globular proteins might be explained by evolutionary pressure to adapt to functional constraints, such as the need for enough conformational flexibility to allow, e.g., induced-fit binding or natural protein turnover, rather than by any intrinsic physical limitations on protein stability. In contrast, the function of adhesive surface fibres requires them to be mechanically resilient, and in the absence of a counteracting evolutionary pressure (e.g., there is no need for protein turnover outside of the cell) no functional constraints on maximum stability apply.

2.2 Fibre Biogenesis

Biogenesis of stable polymeric surface fibres such as those of pili, fimbriae, or capsules, poses many challenges to the Gram-negative bacterial cell. It must be able to protect the unstable and highly aggregative fibre subunits from aggregation and proteolytic degradation during their transport from the site of production in the cytoplasm, across the inner membrane (IM) and the periplasm, to the site of assembly at the outer membrane (OM) of the cell. Having reached the OM, subunit assembly must be controlled to form the desired polymeric structure, which must then be secreted to the cell surface. In the cytoplasm, pilin subunits are expressed as preproteins with an N-terminal export signal that targets them for export via the general secretion (Sec) pathway [50]. In the periplasm, a periplasmic chaperone,

together with an OM usher, handle the subsequent events that lead to assembly of pilin monomers into surface located fibrillar structures (Fig. 2).

The periplasmic chaperones are steric chaperones that bind to fibre subunits as they emerge in the periplasm, ensure their correct folding, and deliver the folded subunits to the usher where they are assembled into fibrillar polymeric structures. For TDA-carrying structures, binding of a chaperone:TDA complex to an empty usher initiates assembly [51–53] which then proceeds by sequential addition of pilin subunits to the base of the growing fibre and simultaneous secretion of the fibre through the usher pore [54]. In the absence of chaperone, subunit folding is slow and leads to a marginally stable and aggregation prone structure [55], whereas in the presence of chaperone, stable and soluble chaperone:subunit complexes are rapidly formed. In contrast to the many ATP-dependent cellular chaperones, the periplasmic chaperones do not require an input of external energy for subunit release (there is no ATP in the periplasm), and organelle assembly is independent of cellular energy [56].

The L-shaped periplasmic chaperones comprise two Ig-like domains joined at ~90° angle, with a large cleft between the two domains (Fig. 5). The F_1 and G_1 β-strands in the 1st, N-terminal, domain are connected by a long and flexible loop that protrudes like a handle from the body of the domain. This loop harbours a conserved motif of hydrophobic residues that is critical for subunit binding. FGL chaperones, used for assembly of SDA polyadhesins such as F1 antigen (Caf1M chaperone), have a relatively long F_1–G_1 loop (hence FGL for F_1–G_1 Long), whereas the FGS chaperones used for assembly of composite structures such as type 1 fimbriae (FimC chaperone) or P pili (PapD chaperone) have a relatively short F_1–G_1 loop (hence FGS for F_1–G_1 Short) [25]. FGL chaperones are also distinguished from FGS chaperones by a longer A_1 strand and a disulphide link bridging the F_1 and G_1 strands.

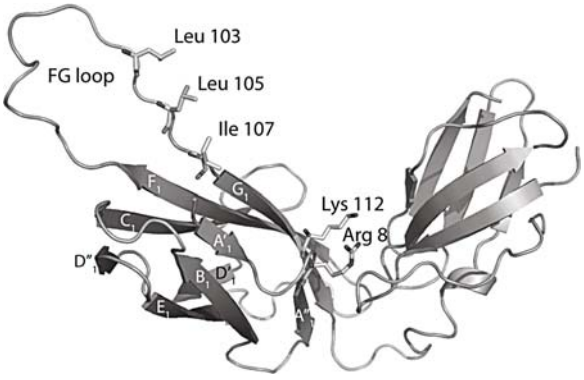

Fig. 5 Chaperone structure. Ribbon diagram of FimC chaperone from the structure of the FimC:FimH complex [32]. β-strands in the N-terminal domain are labelled. The hydrophobic residues in the G_d donor strand are shown as stick models and labelled. Also shown are the two invariant residues in the subunit binding cleft between the two Ig-fold domains that are crucial for subunit binding and chaperone function

Subunits bind in the cleft between the two chaperone domains (Fig. 6) with the subunit C-terminal carboxyl group anchored by two positively charged residues (Arg8 and Lys112 in FimC) at the bottom of the subunit-binding cleft (Fig. 5). These two residues are strictly conserved in all the periplasmic chaperones and are crucial for chaperone function [25, 58, 59]. As described above, the incomplete fold of pilin subunits precludes the formation of a closed hydrophobic core, leaving a surface-exposed hydrophobic cleft between the two sheets at the AF edge of the subunit (Figs. 3 and 4). In chaperone:subunit complexes, the A and F edge strands are hydrogen bonded to the A_1 and G_1 strands of the chaperone, which creates a super-barrel of β-strands from both the subunit and the chaperone [35]. In the super-barrel, large hydrophobic residues from the G_1 donor strand of the chaperone are inserted between the two sheets of the subunit β-sandwich and become an integral part of the bound subunit's hydrophobic core (Fig. 4b). The large hydrophobic donor side chains of FGS chaperones occupy sub-pockets P1–P3; a conserved asparagine side chain binds in the P4 pocket [32, 33]. FGL chaperones donate small hydrophobic side chains to all five sub-pockets in the acceptor cleft [35, 39]. The chaperones thus cap the hydrophobic polymerization cleft, thereby preventing both premature assembly and unspecific subunit aggregation, and protecting subunits from proteolytic degradation. It should be noted that, in contrast to the DSC interaction between subunits in an assembled fibre, where the subunit G_d donor strand is inserted antiparallel to the F strand to create a complete canonical Ig module, the chaperone G_1 donor strand is inserted parallel to the F strand.

Periplasmic chaperones deliver folded pilin subunits to the OM usher. At the usher, chaperone:subunit interactions must be replaced by subunit:subunit interactions. Hence, the A_1 and G_1 strands of the chaperone capping the subunit at the base of the growing structure, on the periplasmic side of the usher, must dissociate to allow the N-terminal sequence of the next subunit to be bound in the polymerization cleft (Fig. 2). This exchange process, called 'donor strand exchange' (DSE) [32–35], can occur even in the absence of usher as evidenced, e.g. by the accumulation of low molecular weight Caf1 polymers in the periplasm of Caf1A usher negative bacteria expressing Caf1M chaperone and Caf1 subunit, or in vitro following incubation of Caf1M:Caf1 complex [43]. However, compared to usher mediated assembly, this process is slow and inefficient, suggesting that DSE assembly is catalyzed by the usher.

Two basic models for DSE have been suggested [35]. In the first model, the chaperone bound to the subunit at the base of a growing fibre is first released, followed by ordering and insertion of the N-terminal G_d donor sequence of the next chaperone:subunit complex into the unoccupied polymerization cleft. The second model involves concerted release of the chaperone G_1 donor strand and insertion of the subunit G_d donor strand in a zip-out-zip-in mechanism. The observation of a transient quaternary complex between two chaperone:subunit complexes during assembly of type 1 fimbriae [39, 60] strongly argues for the second model. Interactions with the P5 acceptor cleft sub-pocket have been shown to be critical for initiation of DSE [39].

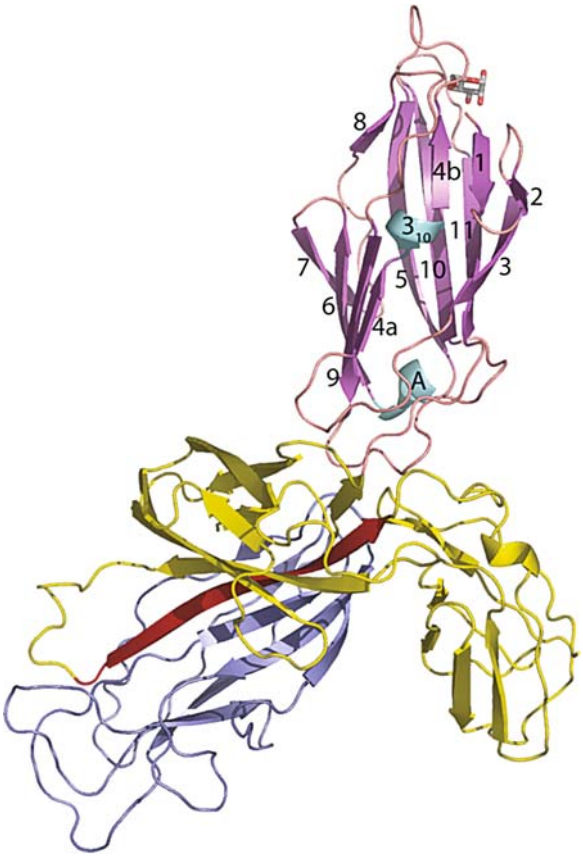

Fig. 6 Crystal structure of FimC:FimH chaperone:adhesin complex bound to α-D-mannose [57], showing the chaperone FimC (*yellow; G_d strand red*), the pilin domain of FimH (*steel-blue*) that is donor-strand complemented by the chaperone G_d strand, and the receptor-binding domain (*violet with blue-green helices*, secondary structure labelled as described earlier [32]). D-Mannose bound to the mannose-binding pocket is shown as a *ball-and-stick model*

No energy input from external sources is required to convert periplasmic chaperone:subunit pre-assembly complexes into free chaperones and secreted fibres [56]. Instead, assembly is driven by subunit folding energy conserved by the chaperone [35, 41]. Comparison of the structure of Caf1 bound to Caf1M, and its structure in the F1 fibre module, revealed a large conformational difference. In the Caf1M:Caf1 super-barrel, the chaperone G_1 donor strand occupies the polymerization cleft, with large hydrophobic residues from the G_1 donor strand inserted between the two sheets of the subunit β-sandwich, preventing them from contacting each other (Figs. 3b and 4b). Molecular dynamics simulations predict that this open, partially folded molten-globule like conformation is not stable and would not be maintained in solution. In contrast to the chaperone donor residues, the much

smaller donor residues in the subunit N-terminal G_d donor segment do not intercalate between the two sheets of the subunit β-sandwich, allowing close contact between them in the fibre module (Fig. 3b). For FGS assembly systems, a similar change accompanies DSE, but now involving a register shift from P1–P4 sub-site binding in the chaperone complex to P2–P5 sub-site binding in the fibre module [34]. A huge difference in stability between the chaperone-bound, partially folded conformation, and the fully folded native fibre conformation of pilins creates a free energy potential that drives fibre formation.

Several observations suggest that periplasmic chaperones target and bind subunits in an unfolded or at least partially unfolded state. The high efficiency of chaperone/usher-mediated assembly in vivo [56] suggests that this process cannot rely on the slow self-folding of subunits [55]. Recently, Vetsch et al. [61] verified that the FimC chaperone indeed binds to unfolded pilin subunits. Chaperone binding was shown to increase the rate of folding by a factor of 100. To bind unfolded subunits, the periplasmic chaperone, presumably, has to recognize some common feature of the (partially) unfolded conformations. The extensive interactions between the hydrophobic cores of the N-terminal domain of the chaperone and the subunit observed in the structures of chaperone:subunit complexes suggest that the chaperone might recognize and attract hydrophobic core residues that are exposed in unfolded subunits. The surface exposed hydrophobic patch created by the bulky hydrophobic side chains in the G_1 donor strand of free chaperones [25, 42] (Fig. 5) might attract (partially) unfolded subunits and provide a template onto which the subunit core can condense, facilitating folding. At the same time, however, because of intercalation of the large chaperone donor residues in the subunit hydrophobic core, subunit folding coupled to chaperone binding does not reach the native state, and the subunit is trapped in an open, activated, high-energy conformation. The resulting meta-stable complex provides a convenient substrate for fibre assembly.

For DSE and secretion to proceed, the usher must interact with chaperone:subunit complexes in the periplasm to facilitate dissociation of the chaperone and polymerization of subunits. The growing polymer must then be translocated across the OM to the cell surface. The ushers are large (80–90 kDa) porin-like integral OM proteins [62–64]. Recent results [52, 65] show that both the PapC (P pilus) and the FimD (type 1 fimbrial) ushers form 7×10 nm^2 homodimers with a ~2 nm pore in the middle area of each monomer. Such a pore is wide enough to allow translocation of folded structural subunits or their polymers through the OM. Functional studies of the PapC and FimD ushers have shown that in addition to a central trans-membrane β-barrel they contain N- and C-terminal periplasmic domains important for initial binding of chaperone:subunit complexes, and subsequent assembly steps respectively [52, 63, 64, 66–68]. Based on an analysis of usher sequences, a third conserved domain located in the central β-barrel region of the ushers has recently been proposed [69]. This 'predicted middle domain' is predicted to have a β-sandwich fold and to be located in the periplasm.

Recently, the structure of a FimC:$FimH_{pilin}$ complex ($FimH_{pilin}$ is the C-terminal pilin domain of FimH) bound to the N-terminal domain of the type 1 pilus usher

($FimD_N$) was reported [68]. The structure of this complex, as well as that of a similar complex from the F1 antigen system (A. Dubnovitsky, A. Zavialov, S.D. Knight, unpublished), shows that the ushers have a chaperone binding surface formed by the folded core of the usher domain and by an extended N-terminal 'tail' of the usher. As we had already predicted in 1996 [25], the usher recognizes a patch of conserved hydrophobic residues on the 'back' of the chaperone N-terminal domain. Whereas in the FimC:$FimH_{pilin}$:$FimD_N$ complex there are also significant interactions between the usher N-terminal tail and the chaperone-bound subunit, very few such interactions are present in the F1 antigen complex. This might reflect the need to distinguish several different subunit types and to assemble these in a particular sequence in the more complex type 1 fimbrial (TDA) system but not in the F1 antigen (SDA) system.

3 Type 1 Fimbriae

Studies of fimbriae have been ongoing since the 1950s. Duguid et al. [70] reported seven different fibrillar structures and named these types 1–6 and F fimbriae. Brinton [71] recognized six different types and named these types I–V and F pili. Duguid's type 1 fimbriae and Brinton's type 1 pili refer to the same fibrillar organelle [22]. Generally, the terms 'type 1 fimbriae' or 'type 1 pili' refer to any 6–8 nm-wide fimbrial structure that mediates agglutination of guinea pig red blood cells in a mannose-inhibitable manner. Such fimbriae are also referred to as 'common', 'somatic', or 'mannose-sensitive' fimbriae. At least two genetically distinct type 1 fimbriae with distinct molecular compositions and receptor binding profiles exist, the *E. coli* type 1 fimbriae (type 1^E) and *Salmonella* type 1 (SEF21) fimbriae (type 1^S) [72]. The focus of this chapter is on the *E. coli* type 1^E fimbriae, which in the following will be referred to simply as type 1 fimbriae.

Type 1 fimbriae are common throughout the *Enterobacteriaceae*. They can easily be visualized in the electron microscope as 1–2 μm long and ~7 nm wide structures extending peritrichiously from the bacterial cell surface (Fig. 1a). They mediate binding to a wide range of glycoproteins carrying one or more N-linked high-mannose structures. Binding can be inhibited by D-mannose and a variety of natural and synthetic oligosaccharides containing terminal mannose residues. High-resolution images show that type 1 fimbriae are composite structures with a short (~20 nm) and thin (2 nm) tip fibrillum at the distal end of the 7-nm fimbrial rod [46]. Type 1 fimbriae are relatively stiff structures (very little bending is observed in electron micrographs of isolated type 1 fimbriae (see, e.g. [47, 71])), but are not rigidly cemented to the cell surface since individual fimbriae can be seen extending at various angles from the cell surface in electron micrographs of type 1 fimbriated bacteria. A structural reconstruction based on electron microscopy and fibre diffraction data [47] shows that the rod of type 1 fimbriae is a right-handed helical structure with 27 FimA subunits in the 19.3 nm helical repeat (eight turns) and a 2.1–2.5 nm-wide central axial hole.

3.1 Genetic Organization and Regulation

The production of type 1 fimbriae requires at least eight genes localized within the *fim* gene cluster and is subject to phase variation (Fig. 7). *fimA*, *fimF*, *fimG*, and *fimH* code for the four protein components of type 1 fimbriae, with a FimA polymer forming the helical rod, and a single FimH TDA strategically located at the distal tip of each fimbriae (Fig. 2) [46]. FimH is attached to the rod via single copies of FimG and FimF, forming the short and stubby tip fibrillum. Assembly of type 1 fimbriae is mediated by the FimC chaperone together with the OM usher FimD (Fig. 2). *fimB* and *fimE* encode regulatory proteins that control the expression of type 1 fimbriae as outlined below. It is currently not clear whether FimI constitutes a structural subunit of type 1 fimbriae or is a regulatory protein, although *fimI* certainly is required for normal fimbrial biosynthesis [74]. Site-directed mutagenesis employed to create lesions in *fimI*, and chromosomal *fimI* mutations, produced fimbriation-negative phenotypes. Minicell analysis associated *fimI* with a 16.4-kDa non-cytoplasmic protein product. It has been suggested that FimI could have a similar function as the PapH protein involved in cell anchoring and length modulation of *E. coli* P pili [75], but this seems unlikely since no effect on fimbrial length or anchoring was observed in the studies by Valenski et al. [74].

Phase variation allows individual bacteria to turn the expression of specific virulence factors on or off. Most of the fimbrial adhesins expressed by *E. coli* are controlled by phase variation and hence only a subset of a bacterial population will express a particular adhesin at any given time. A high level of fimbriation triggers inflammatory host responses, putting the entire bacterial colony at risk of being eliminated. Lowering the proportion of fimbriated bacteria decreases the inflammatory response to levels where it may even be beneficial for the pathogen colony [76]. The proportion of bacteria expressing a particular fimbrial adhesin can be influenced by a number of environmental factors such as temperature, pH, osmorality, or the presence of specific ligands in the surrounding medium. Phase variation of type 1 fimbrial expression in *E. coli* is controlled by the site-specific recombination of a 314-base pair invertible element [77], or *fim* switch (Fig. 7b). The *fim* switch is a transcriptional control element of type 1 fimbrial expression. It contains the promoter for the *fimA* gene encoding the major subunit of type 1 fimbriae. The site-specific recombinases FimB and FimE recognize the 9-base pair inverted repeats

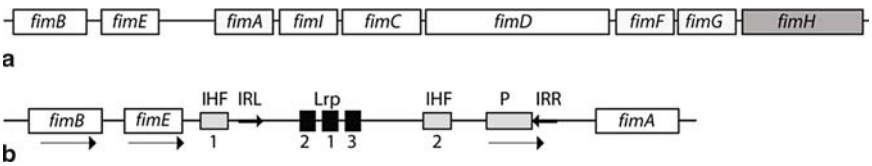

Fig. 7 **a** *fim* gene cluster. **b** Schematic drawing of the *fim* locus with the *fim* switch in the ON (*fimbriate*) orientation and recombinase genes. The direction of transcription of the genes is shown (*arrows*). Lrp, leucine-responsive regulatory protein; IHF, integration host factor; IRL, inverted repeat left; IRR, inverted repeat right; P, *fimA* promoter [73]

flanking the *fim* switch. FimB facilitates inversions in both directions, while FimE can only promote switching from the ON to the OFF phase [78]. In the ON phase orientation, the promoter is correctly oriented for transcription of *fimA* and the rest of the *fim* gene cluster, whereas in the OFF orientation there is no transcription [79]. The predominance of FimE results in the preferential rearrangement of the element in the OFF phase orientation [80]. The genome of the pyelonephritis isolate CFT073 [81] contains genes for three unlinked, FimB- and FimE-like (~50% amino acid sequence identity) tyrosine site-specific recombinases [82]. At least one of these, IpuA, is active at its native chromosome location and can switch *fim* both ways independently of FimB and FimE. A second recombinase, IpbA/HbiF, which appears to be relatively common in commensal, UPEC, and meningitis-associated *E. coli* strains [82, 83], promotes OFF to ON switching to maintain a locked ON phenotype when overexpressed in trans. The suppression of HbiF activity (preventing a locked ON phenotype) in the meningitis isolate RS218 appears to be required to obtain a high degree of bacteraemia in neonatal rats [83].

In addition to the *fim* recombinases, efficient inversion of the *fim* switch requires accessory global regulators like integration host factor (IHF), leucine-responsive regulatory protein (Lrp), and histone-like nucleoid-structuring protein (H-NS). IHF binds with high affinity to two sites, one upstream of and one inside the *fim* switch, to promote switching by FimB (100-fold) and FimE (15,000-fold) [84]. Mutations in the IHF binding sites lower the affinity of IHF binding in vitro and the frequency of FimB and/or FimE recombination in vivo. The presence of the global regulator Lrp is required for normal inversion of the *fim* switch in vivo. Lrp binding increases both FimB and FimE recombination in vivo by binding with high affinity to two of the three sites (1 and 2) within the *fim* switch [85]. This is a rare example of positive Lrp-mediated regulation. Lrp-mediated activation is enhanced by branched side chain aliphatic amino acids, in particular leucine, and also by alanine. Binding of Lrp to its third site inhibits recombination [86]. H-NS down-regulates expression of *fimB* and *fimE* in a temperature-dependent manner, with opposite effects at 30 and 37 °C, by binding to the regions containing the *fimB* and *fimE* promoters respectively [87]. The temperature-dependent H-NS activity modulates type 1 fimbrial expression to favour a fimbriated state at the mammalian body temperature.

As a consequence of host defences against bacterial infection, both sialic acid and GlcNAc release from the host is enhanced. These two potentially key indicators of host inflammation regulate type 1 fimbrial phase variation to inhibit fimbriation through the NanR (sialic acid responsive) and NagC (GlcNAc-6P responsive) regulators [88–90]. NanR targets an operator located over 600 bp upstream of the *fimB* promoter. Binding of NagC to its two operator regions, one close to the NanR binding site and one 212 bp closer to the *fimB* promoter, is enhanced by IHF binding to a site located between the two NagC binding sites. In the absence of sialic acid and GlcNAc, NanR and NagC bind to their operator sites to stimulate FimB expression and promote switching to the fimbriated state. In the presence of sialic acid or GlcNAc/GlcNAc-6P, binding is lost, favouring the non-fimbriated state. Possibly, the ability of *E. coli* to sense the inflammatory host response and to in turn respond by down-regulating expression of type 1 fimbriae can help the infecting bacteria to circumvent host defences by balancing host-parasite interactions.

Numerous examples from recent work demonstrate that the expression of different cell surface structures by bacteria is co-ordinately controlled and often mutually inhibitory [91–93]. Bacteria coordinate gene expression at the single cell level to prevent co-expression of different types of fimbriae. P or S fimbrial expression in clinical isolates leads to type 1 fimbrial repression, through the activity of PapB and SfaB respectively [94, 95]. A mutant of the CFT073 *E. coli* strain incapable of expressing either type 1 or P fimbriae compensated by synthesizing F1C fimbriae [96]. The study by Snyder et al. [96] also showed for the first time that the type 1 vs P fimbrial cross-talk works in both directions and that inversely coordinated expression of adhesin gene clusters also occurs in vivo. Phase variation and coordinated regulation are presumably employed by the pathogenic bacteria to adapt to sequentially changing environments during infection, colonization, and/or invasion [97].

3.2 Role in Disease and Biofilm Formation

Type 1 fimbriae have a well established role in UTI [98], and have also been implicated in neonatal meningitis [99], Crohn's disease [100, 101], and bovine mastitis [102–106]. Their involvement in UTI pathogenesis has been extensively studied. UTIs are believed to affect at least 50% of women in the western world over their lifetime. Each year, 150 million UTIs have been estimated to occur worldwide. The most common cause of UTI in humans is UPEC infection, accounting for about 80% of reported cases. UPEC-caused UTI is also common in animals, e.g. cats and dogs [107].

The expression of mannose-specific type 1 fimbriae on the cell envelope of UPEC allows for the attachment to the epithelium of the bladder and the lower urinary tract. This leads to fast colonization rates, resulting in lower urinary tract infections (cystitis). Binding is crucial for efficient infection, and blocking adhesion has been shown to prevent cystitis [12–14, 16, 108]. However, type 1 fimbriae trigger inflammatory host responses and stimulate the production of proinflammatory cytokines including IL-6, IL-8, and TNF-α [109–111]. Hence, the ability to control the degree of fimbriation in a colony through phase variation (see Sect. 3.1) is important for successful colonization. In general, UTI can be treated with antibiotics, such as trimethoprim sulfamethoxazole, fluoroquinolone, nitrofurantoin and fosfomycin. However, both the rise of antibiotics resistance [6–8] and the recurrent nature of UTIs [112] are worrisome. Approximately 25–35% of initial UTI episodes recur within 3–6 months, and in about two thirds of the cases the recurrent infection involves reinfection by the same bacterial strain that caused the primary infection. During the past decade, Hultgren's group unravelled the mechanisms responsible for recurrent UTI [113]. Contrary to what was previously believed, UPEC can invade into the epithelium lining the bladder and lower urinary tract, the urothelium [15, 114]. Invasion is triggered by binding of type 1 fimbriae to the uroplakin complexes that cover the luminal surface of the urothelium (see Sect. 3.3). Following invasion, most UPEC strains are able to form large intracellular bacterial

communities (IBCs) that eventually mature into a slow-growing, biofilm-like organisation of coccoid-shaped bacteria [115, 116]. Bacteria in these IBCs are protected from antibiotics and the immune system of the host, and in some hosts can persist for months in a dormant and antibiotic-insensitive state [117]. Despite invasion and intracellular replication being relatively rare events, the successfully invasive bacteria rapidly produce progeny of about 500 bacteria per IBC. Within a few hours, the progeny bacteria escape from the matured IBC [118], (re)invade host cells, and reinitiate the IBC cascade [98]. Very little is known about type 1 fimbrial gene regulation during the different stages in the pathogenic cascade of recurrent UTIs. However, since initiation of UPEC biofilm formation on abiotic surfaces is dependent on type 1 fimbriae [119], it remains an intriguing question whether they are also expressed in the IBCs.

Biofilms consist of surface-associated colonies of bacteria and are a major concern for implanted medical devices and in many diseases [120–122]. Bacterial biofilms are highly organized communities embedded in an exopolysaccharide matrix, and contain several layers of bacteria with distinct functions. Biofilms grow slowly but efficiently to coat abiotic surfaces, and can eventually almost completely fill up narrow tubing. Because of the entrenched structure of biofilms, an antibiotic cannot penetrate deeply enough into the distant parts of the biofilm to kill all bacteria. Therefore, biofilms are difficult to remove mechanically or by means of antibiotics or disinfectants.

Biofilm formation is a complex process involving adhesion, aggregation, and expansion of the bacterial community, and requires the careful orchestration of gene expression to co-ordinately activate the multiple cellular mechanisms involved in establishment, development, and maintenance of the bacterial community [121]. The first crucial step in biofilm formation is adhesion. Type 1 fimbriae are critical for formation of *E. coli* biofilm on abiotic surfaces, including polyvinyl chloride, polypropylene, polycarbonate, polystyrene, and borosilicate glass, and the initial attachment is mannose-inhibitable [119]. On the other hand, the adhesin appears not to be strictly necessary for biofilm formation [123]. Type 1 fimbriae without the FimH TDA also facilitate immunoglobulin-mediated (secretory immunoglobulin A and IgM) biofilm formation by *E. coli* on polystyrene. Nevertheless, biofilm formation is more pronounced for bacteria with type 1 fimbriae that carry the adhesin, and it is arguable whether FimH-lacking type 1 fimbriae are really expressed on the cell envelope of clinical isolates of *E. coli*.

Following adhesion and establishment of an adhered bacterial community, further biofilm development requires tight interactions between individual cells in the community. In *E. coli*, the product of the *flu* gene, Ag43, mediates auto-aggregation of bacteria and micro-colony formation [124, 125]. Ag43-induced auto-aggregation cannot take place in the presence of type 1 fimbriae [124], and the expression of fimbriae and Ag43 are co-ordinately controlled [126].

The extent to which the factors that are important for biofilm formation on abiotic surfaces are also important for biofilm formation on biotic surfaces (e.g. in uroepithelial IBCs) is not known, and needs to be studied further. The observation of bacterial biofilm formation on abiotic surfaces mediated by (glyco)proteins [123] is highly

relevant in view of the use of medical implants such as urinary catheters. In particular, the mannosylated Tamm-Horsfall protein (THP) (previously called uromodulin) is secreted in urine as a natural inhibitor of type 1 mediated bacterial adhesion [127] (see Sect. 3.3). Glycoproteins such as THP could coat the catheter walls and serve as glue for type 1 fimbriated *E. coli* to initiate biofilm growth.

3.3 Receptors in the Urinary Tract

The urothelium is a highly specialized endothelium covered almost completely with uroplakins. The most abundant glycoprotein receptors for FimH in the lower urinary tract are uroplakins UPIa and UPIb [128, 129]. These are integral membrane proteins that, together with UPII and UPIII, form ring-shaped complexes with a central 3.7 nm wide cavity in the highly differentiated superficial cell layer of the bladder [130, 131]. Electron microscopy of FimH added to asymmetric unit membranes of the bladder provided evidence that FimH binds to the inner six sub-domains of the 16-nm uroplakin particles, at the sites where UPIa is located [132]. Under quick-freeze, deep-etch electron microscopy, the type 1 tip fibrillae appear to be at least partially buried in the central region of the uroplakin complexes [15]. This suggests that the high-mannose chains on UPIa are exposed on the surface of the central cavity of uroplakin complexes, and that binding is accompanied by (partial) insertion of the tip fibrillum into the cavity. The interaction of FimH with terminally exposed mannose residues on UPIa can lead to severe consequences for the targeted host cells, including bacterial uptake and internalization (see Sect. 3.2).

Recent mass-spectrometric determinations revealed that, like mouse UPIa, human UPIa also carries high-mannose chains while human UPIb only carries complex type glycans [133]. These findings established the concept that UPIa is the major urothelial receptor in humans and other mammals. The determination of uroplakin glycans has been technically challenging due to the difficulty in isolating the highly insoluble uroplakins individually (the uroplakins form a tight complex with each other in the epithelial membrane) and because of the complexity and heterogeneity of the carbohydrates. Mouse and human UPIa are very similar in their glycosylation and hence FimH binding, validating the use of mice as an in vivo UTI model [116]. Interestingly, small differences in the glycosylation of UPIb from bovine vs mouse or human leads to detectable FimH binding of the bovine UPIb, but not to human UPIb [133]. It remains to be seen whether the glycosylation of human UPIa, determined here from cells of 14–16 week old embryonic bladders, is age-dependent. It is interesting to note that β-galactosidase activity is a marker for senescent human cells in culture and aged skin cells in vivo [134], and also marks the senescence, increasing sharply during 25–40 days of age, of normal human urothelium in an organ-like culture [135]. A 40-week period typically represents the turnover rate of differentiated cells in the bladder of mice [136]. The enzyme β-galactosidase cleaves terminal galactose residues from complex glycans, which together with *N*-acetyl glucosaminidase activity would lead to exposure of terminal mannose

residues. Such activity could potentially make UPIb on aged human cells susceptible to FimH binding and adherence of uropathogenic bacteria.

Binding of type 1-fimbriated UPEC to high-mannose moieties on THP inhibits uroplakin binding and it has been suggested that it is an important host defence mechanism [137]. THP is a heavily glycosylated GPI-anchored protein located on the cells lining the thick ascending limb of Henle's loop in the kidney. A specific protease cleaves THP and releases large amounts into the urine (~50 mg day^{-1} in urine from healthy human individuals), making it the most abundant protein in normal human urine. THP knock-out mice have been shown to be more prone to bladder infection by type 1 fimbriated UPEC [138, 139]. There are seven *N*-glycosylation sites in THP, of which one, Asn251, carries high-mannose carbohydrate chains [140]. In humans, the most abundant glycoform is Man6 (75%), followed by Man7 (17%) and Man5 (8%) [127]. Man5 is the only one of these glycoforms that exposes Manα1–3Manβ1–4GlcNAc at the non-reducing end of its high-mannose D1 arm. In pigs, the most abundant glycoform is also Man6 (53%), but the Man5 content is much higher (47%) than in human THP. Pig THP binds about threefold better than human THP to type-1 fimbriated *E. coli* [127], consistent with our finding that glycan structures exposing the Manα1–3Manβ1–4GlcNAc epitope provide the tightest FimH binding [141].

3.4 The FimH Adhesin

Adhesion of UPEC as well as other strains of *E. coli* to physiological receptors or other surfaces displaying mannose-containing receptors depends on the FimH TDA located at the tip of type 1 fimbriae. The first crystal structure of FimH was determined in complex with its periplasmic chaperone, FimC [32]. This structure clearly demonstrated that FimH is divided into two domains; a receptor-binding, or lectin, domain, and a pilin domain (Fig. 6). The latter is needed to connect FimH to FimG, which is incorporated in the tip fibrillum of type 1 fimbriae after FimH. The two domains of FimH are coupled through a very flexible linker (J. Bouckaert, unpublished results) made of two glycine residues, Gly159 and Gly160. These precede the third conserved cysteine (Cys161) that makes a disulphide bond (to Cys187) within the pilin domain.

The FimH receptor-binding domain was originally described as an 11-stranded β-barrel, with a fold unrelated to any other protein fold known at that time [32]. With the second and third three-dimensional structures of TDA receptor-binding domains, from PapG-II [142] and F17G [143], becoming revealed, the overall similar fold among these structures became apparent (Fig. 8). From then on, the receptor-binding domains have been characterized as Ig folds, with large structural variation in the loops joining the Ig core made up of strands B, C, E, and F [143]. The pilin domain of TDAs has the same fold as pilin subunits with an incomplete Ig sandwich lacking the 7th, G, strand. Hence, FimH comprises one complete and one incomplete Ig fold. In the receptor-binding domain, the G strand leads directly into

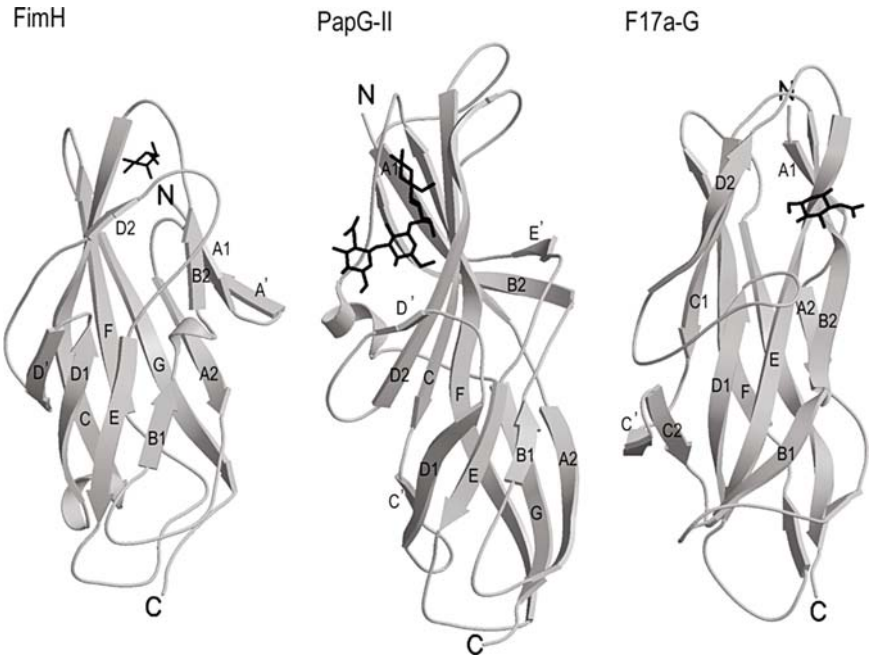

Fig. 8 The receptor-binding domains of three TDAs, FimH [57], PapG-II [142], and F17a-G [143], viewed in the same orientation (obtained by superimpositioning of the structural core of their Ig-fold). The receptor binding sites are in complex with α-D-mannose, globotetraoside, and *N*-acetyl glucosamine, respectively, shown as *black ball-and-stick models*. Structurally equivalent β-strands are labelled with their Ig-fold names

the double-glycine linker (Gly159 and Gly160) that joins the receptor-binding domain to the FimH pilin domain, and is the structural equivalent of the donor strand in the pilin fibre modules. SDA polyadhesins sometimes incorporate a specialised 'invasin' at the very tip of the fibrillar structure [36, 144, 145]. To trigger invasion, an invasin must bind to and interact with target receptors, and so is also an adhesin. Invasins have the same basic fold as pilins but lack an N-terminal polymerization sequence and hence, like the TDAs, can only be located at the tip of the fibre. FimH, which has the dual role of binding and triggering invasion (see Sect. 3.2), might then be thought of as a special case of invasin molecule where a binding/invasin domain is covalently coupled to a pilin domain, rather than linked via DSC as in the polyadhesins.

3.4.1 The Mannose-Binding Pocket

In the FimC:FimH crystals, the receptor-binding domain of FimH was found to have bound to the open ring sugar glucamide of cyclohexylbutanoyl-*N*-hydroxyethyl glucamide (C-HEGA) [32]. C-HEGA had been added at 300 mM to the crystallization

medium in order to improve crystal quality, but was not known to bind FimH. Its binding led to the identification of the mannose-binding pocket, delineated by the loops between β-strands 10 and 11, and between 4 and 5, forming an upper ridge around the binding site, and the β2-β3 loop forming the lower ridge (Fig. 9a). In the crystal structure of the FimC:FimH complex, the glucamide part of C-HEGA was bent in a way to approximate closely the cyclic pyranose ring. Later, the structure of the FimC:FimH complex bound to d-mannose confirmed that C-HEGA had bound in a way that mimicked binding of mannose [57].

Mutation of the amino acids interacting with C-HEGA to alanine or closely resembling amino acids almost uniformly led to complete abolishment of type 1 mediated bacterial haemagglutination, bladder cell binding and bladder tissue colonization [57]. The mutagenesis study gave the insight that the contribution of each single amino acid in the binding pocket is almost uniformly crucial for mannose binding, implying that the recognition by FimH is highly fine-tuned and specific. Furthermore, it showed that modification of the FimH binding pocket directly affected type 1 mediated bacterial adherence to its physiological target, the urothelial mannosylated receptors.

The mannose-binding pocket is a small, deep and negatively charged pocket at the tip of the FimH adhesin (Fig. 9b). Bound mannose makes direct hydrogen bonds to the side chains of residues Asp54, Gln133, Asn135, and Asp140, to the positively charged amino terminus, and to the main chain of Asp47 (Fig. 9c). There are also indirect water-mediated hydrogen bonds from O2 of mannose to the side chain of Gln133 and to the main chain oxygen of Phe1 and Gly14. The water molecule mediating these contacts fills up the space between O2 of mannose and the Phe144 side chain that together with the side chain of Ile13 defines the bottom of the binding site. A collar of hydrophobic residues extends from the mannose-binding pocket towards the tip of the FimH molecule. The high ridge of the collar is bordered by two tyrosine residues, Tyr48 and Tyr137, referred to as the tyrosine gate [147]. These structural features of FimH explain the relatively strong binding of aromatically substituted mannose residues, such as *p*-nitrophenyl mannopyranoside and methyl umbelliferyl mannopyranoside. The hydrophobic collar around the binding site directs the electrostatic attraction forces for binding of the polar mannose residue into the small and charged mannose-binding pocket. The aromatic groups of ligands can pack on the broad hydrophobic platform between the tyrosine rings. This feature is also important for tight binding of alkyl mannosides. In a study based on the unexpected finding of a tight-binding butyl mannoside in the mannose-binding pocket of FimH [147], it was shown that linear alkyl chains on mannose increase the affinity for FimH beyond these for the aromatically substituted mannose. In addition to a strongly hydrophobic nature, the alkyl chains retain significant conformational freedom while interacting to the broad hydrophobic platform of the tyrosine gate, as illustrated by the two alternative bound conformations observed in the two independent crystal structures obtained for the FimH:butyl mannoside complex [147]. This conformational freedom could counteract the entropic cost upon binding of these relatively flexible ligands, thereby significantly enhancing affinity.

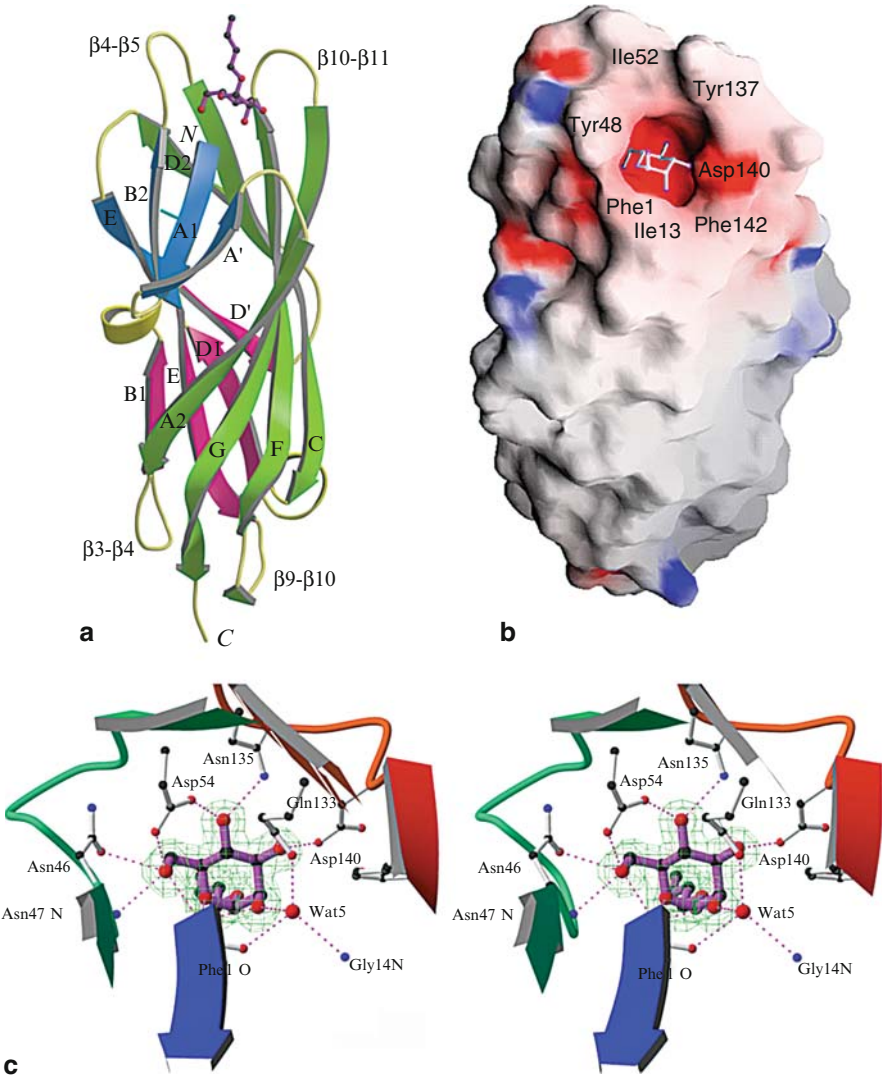

Fig. 9 **a** The three-dimensional structure of the FimH receptor-binding domain is an elongated 11-stranded β-barrel with an Ig-fold. Numbering is according to conventions established for antibody domains [146] and for PapD [33] and loop identifications according to previous descriptions (reference strand numbers A1 = 1, A' = 2, A2 = 3, B1 = 4, B2 = 4', C = 5, D1 = 6, D' = 7, D2 = 8, E = 9, F = 10, G = 11) [32, 57]. The bound saccharide is butyl α-D-mannose [147]. **b** The receptor-binding domain of FimH displaying the electrostatic potential surface [148], with positively charged residues shown in blue, negatively charged residues in red and neutral and hydrophobic residues in white. The residues of the hydrophobic ridge around the mannose-binding pocket are labelled. **c** Stereo image of the mannose binding pocket, viewed 90° away from the orientation in Fig. 9a, and seen from the inside of FimH. The $2F_o–F_c$ electron density for butyl α-D-mannoside is shown. FimH can make 14 possible hydrogen bonds (*purple broken lines*) with the non-reducing mannose. The only oxygen of mannose that is not involved in direct interaction with FimH is the axially oriented O1, sticking outwards of the pocket and in this structure linked to butyl. This agrees with the receptor binding site of FimH being able to bind only to terminally exposed mannose residues on high-mannose glycans [149–153]. A reprinted from [147] with permission from the publisher. B reprinted from [57] with permission from the publisher

3.4.2 Mannose Specificity and Affinity

Analyses of FimH receptor specificity have mostly been performed by using whole fimbriated bacteria. For a few years now it has been possible to compare these results with those of the isolated and soluble receptor-binding domain of FimH (residues 1–158). The same solution affinity equilibrium constants for FimH binding to a series of carbohydrates were obtained in both a surface plasmon resonance (SPR) assay using a monoclonal antibody directed against the mannose binding pocket of FimH, and a tritiated mannose displacement assay [147]. In these binding studies, FimH was confirmed not only to be highly specific, but also to have an unusual high affinity (K_d = 2.3 μM) for mannose. This result had already been indicated from the crystal structure of the FimH-mannose complex, because of the very tight network of hydrogen bonds involved in mannose binding, with in total 14 potential hydrogen bonds involving all of the mannose's oxygen atoms except for the α-anomeric O1 atom [57]. Of all the tested mono- and disaccharides other than mannose (methyl 2-deoxy-α-d-mannopyranoside, glucose, galactose, fructose, sucrose, and turanose), only fructose has an affinity approaching that of FimH for mannose, binding with only 15-fold lower affinity. The relatively tight binding of fructose is presumably due to ring opening and conversion to the pyranose form of fructose (Fru_p). Modelling predicts that Fru_p is differently oriented in the binding site compared to mannose (Fig. 10), allowing it to bind with only one hydrogen bond less than mannose. This hydrogen bond is replaced by a hydroxyl-methyl group interaction. Similar observations of the compatibility between mannose and fructose binding have been made in crystal structures of the bacterial lectin LecB, also named PALII, from *Pseudomonas aeruginosa* [154], the legume lectin from *Pterocarpus angolensis* [155], and the HIV gp120 antibody 2G12 [156].

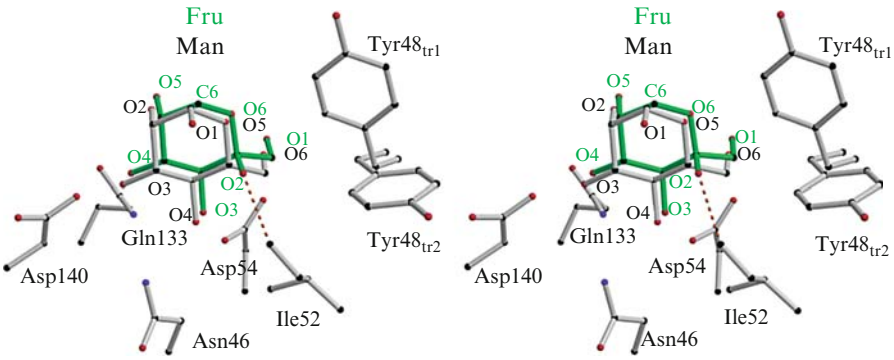

Fig. 10 Fructose superimposed on mannose in the FimH binding pocket. Fructose in *green* (for clarity of the picture, each atom was shifted 0.3 Å from the ideal superposition), mannose in *grey*. The two different Tyr48 side chain conformations are shown. Note the lack of O1 of mannose (anomeric oxygen) and the presence of (an extra) hydroxyl on C2 (the equivalent of C5 of mannose) that is in close contact (2.7 Å) with Ile52 (*orange dashed bond*)

3.4.3 Recognition of Oligosaccharides and Fine Specificity

The physiological receptors for FimH are *N*-glycosylated proteins carrying high-mannose structures. The largest high-mannose glycan, oligomannose-9 (Fig. 11), is fully substituted with terminal α1–2 linked mannosides on its D1, D2, and D3 arms. It has long been known that only mannose at the end of such an arm can bind in the mannose binding pocket of FimH. In oligomannose-9, all three terminal mannose residues at its non-reducing ends are potential candidates for binding in the monosaccharide-binding pocket of FimH. The affinity indeed increases with a factor of three for oligomannose-9 over Manα1–2Man, which at the same time indicates that the binding of oligomannose-9 is not polyvalent. Thus not all three terminal residues are bound simultaneously by one FimH molecule, but the probability to encounter Manα1–2Man has been increased threefold. Prolongation of Manα1–2Man at its reducing end, as in Manα1–2Manα1–2Man, increases affinity only moderately and is glycosidic linkage-independent. These findings suggest that a complementary fit of the larger trisaccharides, providing more hydrogen bonds, more van der Waals interactions and burial of hydrophobic surface, is important for generating tighter binding.

The group of Sharon first observed that other, higher-affinity epitopes, are hidden in oligomannose-9 and are only accessible in high-mannose substructures much smaller than oligomannose-9 [149, 150, 157]. Probing the fine specificity of FimH for high-mannose epitopes using a series of oligomannosides, corresponding to substructures of high-mannose N-linked glycans on proteins, revealed that for those oligomannosides (oligomannose-3 and -5) where the D1 arm is not capped at the non-reducing end by an α1–2 linked mannose residue (Fig. 11) [158], the affinity is very high (K_d = 20 nM) [147]. This affinity parallels the affinity of FimH for aryl (*p*-nitrophenyl α-D-mannose K_d = 44 nM and methyl umbelliferyl α-D-mannose K_d = 20 nM), and alkyl mannosides (pentyl α-D-mannose, K_d = 25 nM, hexyl α-D-mannose, K_d = 10 nM, and heptyl α-D-mannose, K_d = 5 nM) [147].

The highest-affinity epitope for FimH, Manα1–3Manβ1–4GlcNAc, is not free for binding to FimH in any of the recently elucidated glycan structures on mouse UPIa [133]. However, a change in the glycosylation of UPIa or other urothelial surface proteins may alter the host susceptibility to UTIs. Interactions of FimH with monomannose in vitro, but not with trimannose (Manα1–3(Manα1–6)Man), correlate with binding to human bladder epithelium, despite the 10-fold higher affinity of FimH for the latter ligand [57]. This may be understood from the fact that mannose residues that can function as FimH mono-mannose receptors are always present at the non-reducing termini (D1, D2 or D3 arm) of any high-mannose glycan substructure. In contrast, trimannose is only accessible at the non-reducing end of oligomannose 7D1, 6, 5, and 3 (Fig. 11). Only very low amounts of oligomannose 6 are found on mouse UPIa, whereas oligomannose 7, 8, and 9 occur in significantly higher amounts [133]. Hence trimannose is available for FimH binding to a much smaller extent than mono-mannose. This is congruent with our previous findings for binding to human bladder tissue of FimH variants with engineered point mutations in the mannose-binding pocket [143]. The binding of recombinant type 1 fimbriated *E. coli* strains to human bladder tissue sections was correlated with mono-mannose binding

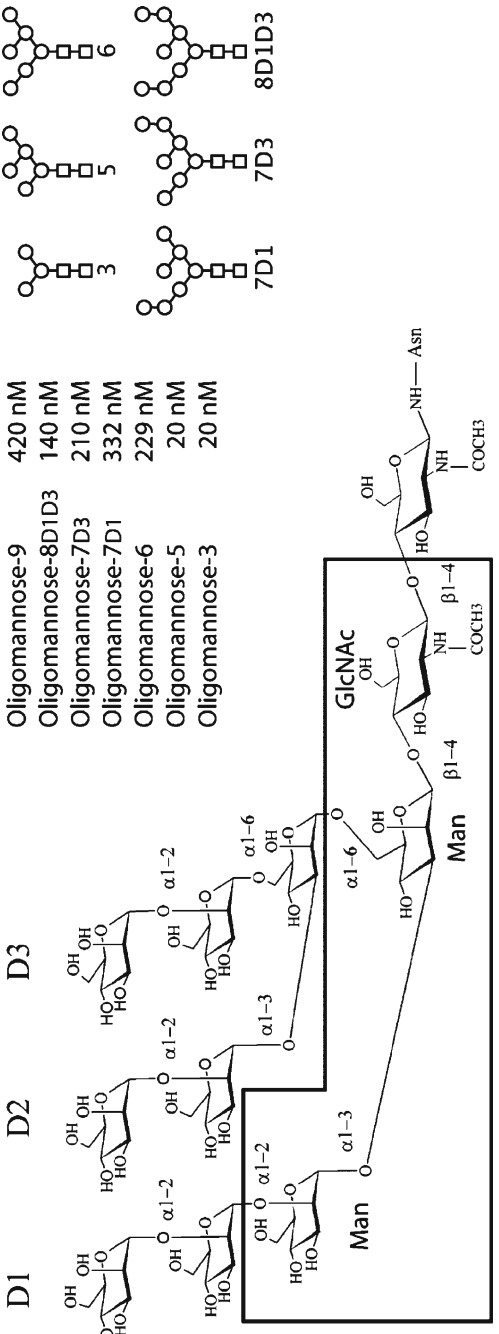

Fig. 11 Epitope mapping on the N-linked high-mannose glycan with FimH on Biacore*3000* reveals the highest affinity (K_d = 20 nM) for the Manα1–3Manβ1–4GlcNAc epitope (boxed) on oligomannose-3 and oligomannose-5, due to the presence of an unsubstituted D1 arm. Structures of the different oligomannoses are illustrated schematically to the right (*squares* = GlcNAc; *circles* = Man)

of the corresponding mutant FimC:FimH complexes, but not with their (tighter) trimannose binding.

There is ample evidence that the carbohydrate expression profile of eukaryotic cells can be subject to variation in certain disease states, but also under normal physiological conditions such as menopause and aging (for a review, see [159]). Interestingly in this regard, diabetic patients are more prone to UTI than otherwise healthy individuals [160]. Twice as many type 1 fimbriated *E. coli* adhere to urothelial cells of diabetic patients than of healthy individuals, even taking into consideration the presence of various substances excreted in the urine, such as albumin, glucose and THP [161]. Unfortunately, it is currently unknown whether this can be attributed to altered glycosylation of FimH receptors in the urinary tract. A better understanding of the fundamental relationships between physiological conditions of the host and carbohydrate expression on urothelial cells is thus needed.

The (limited) allelic variation in FimH [57] between *E. coli* clinical isolates from intestinal or extra-intestinal origin, mainly from the urinary tract, has long been though to affect directly the structure and function of the FimH receptor-binding domain. Type 1 fimbriated bacteria from different *E. coli* clinical isolates display altered mannoside binding and adhesion profiles. Recombinant *E. coli* expressing the CI#4 (UPEC) FimH variant adhere tightly to yeast mannan, A498 human kidney cells, and J82 human bladder cells, whereas bacteria expressing FimH from the fecal *E. coli* F-18 strain show poor adhesion to all three substrates [162]. The F-18 strain only adheres under shear conditions in parallel flow chambers, and its cells do not agglutinate guinea pig red blood cells under static conditions but only co-aggregate under rocking [163]. Minor sequence variations in FimH have been held responsible for these functional differences [162, 164–166].

Recent affinity measurements using the isolated FimH receptor-binding domain originating from a number of different strains, including UPEC, commensal *E. coli*, and EHEC strains, contradict this hypothesis [141]. The FimH receptor-binding domains from two UPEC, one fecal, and three EHEC strains have identical affinities for mannose and a series of high-mannose glycans and high-mannose substructures (the only exception to this is the FimH domain from some EHEC strains that have a Lys instead of an Asn residue at position 135 in the binding pocket, abolishing all binding). As an example, our data show that there are no significant differences in the affinities for d-mannose or trimannoside between the FimH from *E. coli* F-18 and from *E. coli* CI#4. Hence, the single Gly73Glu amino acid difference between these two FimH variants does not have a direct effect on affinity. This suggests that factors other than differences in mannose binding of FimH per se cause the different adhesion phenotypes.

Factors that might influence adhesion properties include the number of fimbriae per cell, the number of fimbriae that are functional for receptor binding, the fraction of cells that are fimbriated, the length and the flexibility of fimbriae, and the ability of fimbriae to deform under the influence of mechanical force. For example, it is up to date not known to what extent variant residues in the FimH receptor-binding domain affect assembly and thus the number of fimbriae on the bacterial cell envelope of bacteria expressing mutant FimH receptor-binding domains. The receptor-binding domain is necessary to initiate pilus assembly by interactions between

the FimH receptor-binding domain and the usher OM export channel [51, 66, 167], and it is not impossible that some of the mutations that affect adhesion target (or indirectly influence the conformation of) residues that interact with the export channel of the FimD usher. For example, the natural variant residue Ala/Val27, a double mutation engineered to inhibit FimH linker strand extension, Gln32Ala/Ser124Ala [163], and the point mutation Val156Pro, engineered to facilitate linker strand extension [163], are all located on the surface of FimH. Hence, the effect of these variations on assembly is worthy of further investigation. Reduced assembly efficiency, resulting in a smaller number of fimbriae, could significantly reduce the possibilities for multivalent binding, as described earlier [168].

The type 1 fimbrial shaft has a strong influence on the affinity and specificity of adhesion [169–171]. For example, type 1 fimbriae from *S. typhimurium*, *K. pneumoniae*, and *E. coli*, exhibit distinct adhesion and haemagglutination profiles. In contrast, FimH molecules from any of these three species bind to a broad range of mannose-containing compounds when expressed as MalE fusion proteins. Intriguingly, the adhesion profile of bacteria expressing hybrid type 1 fimbriae (e.g. *K. pneumoniae* FimH at the tip of *E. coli* type 1 fimbriae or vice versa) resembles the adhesion profile of the bacteria from which the fimbrial rod was derived [171]. Electron microscopic pictures have revealed that the helical rods of type 1 fimbriae and P pili can extend significantly as a result of either mechanical shear during preparation [172], or from exposure to 50% glycerol [173]. The extension is due to breaking of the quaternary interactions between non-adjacent pilin subunits within the right-handed helical rod, leading to its uncoiling. Extension of fimbriae in response to shear was suggested to allow an increased number of fimbriae of a bacterium to adhere simultaneously, thereby increasing the strength of adhesion [174]. Recent work using optical tweezers demonstrates that the unfolding of the helical structure of P and type 1 fimbriae to a linear conformation is fully reversible and that the fimbrial rod can work as a spring under shear forces [175–177]. The spring-like qualities of the rods have been suggested to be fine tuned to support the formation of long-lived catch bonds that promote tight adhesion under conditions of high shear stress [177] (see Sect. 3.5.2). Since there is much more sequence variability between structural subunits in different *E. coli* strains than between TDAs, rod properties can be expected to vary considerably. In contrast, different FimH variants have been shown to have indistinguishable binding properties [141]. Hence, differences in adhesive properties are most likely due to different rod properties caused by sequence differences between rod subunits (FimA in the case of type 1 fimbriae).

3.5 Factors that Enhance Adhesion

3.5.1 Multivalency

The presence of multiple fimbriae on the cell surface allows bacteria to adhere to target surfaces by simultaneously using multiple and often weak, non-covalent protein-carbohydrate interactions between the adhesin and its receptor. Such

multivalent binding significantly increases the adhesive forces and is the reason why even relatively weak adhesin-receptor affinities can provide considerable binding strength. Studies of adhesion of type 1 fimbriated *E. coli* to self-assembled monolayers (SAMs) displaying α-C-mannoside ligands have revealed that both the relative orientation of bacteria towards the binding surface, and the density of receptors on the surface, strongly influence the number of fimbriae that are involved in bacterial attachment and hence the strength of adhesion [168]. Side-on attachment of the elongated *E. coli* bacteria leads to strong polyvalent interactions mediated by multiple fimbriae, whereas in end-on attachment, achieved by manipulating the bacteria with optical tweezers, only one or two fimbriae simultaneously are able to find an accessible mannose ligand, resulting in relatively weak adhesion. This effect is much more pronounced for binding to a high-density SAM (4×10^5 ligands μm^{-2}) compared to a SAM with a low (4 ligands μm^{-2}) surface density of mannose. In the experimental set up of Liang et al. [168], the force required to remove a bacterium attached side-on to the SAM varied between 3.5 to ≥18 pN (high-density SAM) and between 3.8 to 7.8 pN (low-density SAM), suggesting that the number of fimbriae involved in adhesion differed from bacterium to bacterium. In some cases, the maximum force available in the apparatus used (18 pN) was not enough to immediately detach bacteria. However, sweeping the position of the optical tweezers across the entire length of the bacterium eventually led to detachment, presumably through sequential dissociation of individual interactions between the α-C-mannoside ligands and FimH receptors in a 'Velcro-like' manner. From repeated measurements of detachment of bacteria attached end-on, the force required to break the interaction between a single type 1 fimbriae and a surface-bound α-mannoside was estimated at 1.7 pN.

3.5.2 Shear-Enhanced Adhesion

Bacterial adhesion often occurs under conditions of shear stress exerted by the flow of liquids (e.g. urine, saliva, mucus) over the binding surface. Although in many cases shear stress counteracts adhesion by limiting binding and washing away unbound bacteria, cases where shear stress increases adhesion have also been observed and might constitute an important factor in bacterial colonization of target tissues. The groups of Vogel and Sokurenko jointly investigated shear-dependent 'stick-and-roll' adhesion of type 1 fimbriated *E. coli* [163, 177–182]. In their parallel flow chamber experiments, bacteria in PBS-BSA solutions were pumped at various flow rates through parallel plates coated with mono-mannosylated BSA [182] or with RNase B (an *N*-glycosylated protein carrying high-mannose structures) [178–180], and video-imaged to follow attachment and detachment from the surfaces. At low flow rates, bacteria were observed to roll along the surface. Presumably, rolling adhesion is caused by the transient formation and breaking of individual FimH-mannose interactions as the bacteria are transported along the glycosylated surface. Moderately high shear was found to enhance the adhesion of type 1 fimbriated *E. coli* to mannose-containing surfaces. With increased flow rate or viscosity, the

bacteria switched from rolling attachment to stationary binding. As expected, at even higher levels of shear stress, the bacteria eventually detached and were washed away. Shear-enhanced adhesion was more pronounced for binding to mono-mannose-coated surfaces than for binding to surfaces displaying trimannose or high-mannose structures. The observed effect of shear on adhesion was also different for different type 1 fimbriated *E. coli* strains expressing different FimH variants, being more pronounced for fecal isolates [163]. In summary, the less specific and hence the lower the affinity is for the receptor, the larger the effect of shear force is on adhesion. Shear-enhanced adhesion was proposed to depend on the formation of so-called 'catch bonds', i.e. bonds that become stronger under application of force [183]. Conformational changes in the FimH mannose-binding pocket caused by shear force-induced extension of the FimH interdomain linker were suggested to promote the formation of catch bonds.

Shear-dependent adhesion may be physiologically relevant, allowing bacteria to move and spread over surfaces at low shear stress levels while keeping them firmly attached at higher shear stress, e.g. during voiding of urine. In particular, the weak, rolling, type of adhesion appears to allow bacteria to more rapidly spread and colonize target surfaces in the presence of moderate fluid flow [178]. In addition, shear-activated adhesion may help protect bacteria from soluble inhibitors present in, e.g. urine (see Sect. 3.3) or administrated as anti-adhesive drugs. Nilsson et al. [179, 180] studied the inhibitory effect of methyl α-D-mannose on binding of type 1 fimbriated *E. coli* to mannosylated surfaces under different shear stress conditions. Type 1 fimbriated *E. coli* were allowed to bind to RNase B-coated flow cell surfaces for 6 min at low (0.25 Pa) shear stress before addition of 400 mM methyl α-D-mannose to the flow solution. At low shear stress levels (≤0.5 Pa), where bacteria exhibit weak rolling adhesion behaviour, the presence of methyl α-D-mannose dramatically increased the rate of bacterial release from the surface. In contrast, almost no detachment was observed when high (4 Pa) shear stress levels, promoting tight stationary adhesion, were applied. The reason for this bimodal behaviour is presumably that during rolling, FimH molecules transiently bind and detach from surface receptors, allowing a soluble inhibitor such as methyl α-D-mannose to eventually bind to all FimH molecules, thereby preventing further adhesion. In contrast, stationary adhesion is mediated by long lived adhesin-receptor bonds that prevent inhibitor binding during the time course of the experiments (~10 min). Nevertheless, the presence of a soluble inhibitor such as methyl α-D-mannose during a longer period of time (hours) can sometimes promote biofilm formation under conditions of low shear by loosening the interaction between statically adhering bacteria and the surface, allowing them to spread by rolling [178]. In conclusion, for a free small-molecule ligand to be an efficient FimH anti-adhesive even under conditions of fluid flow, it must bind significantly tighter to FimH than the receptor molecules to overcome the shear-enhanced affinity. In this context it is interesting to note that whereas human uroplakin UP1a exposes mainly mono-mannose receptors [133], human THP (see Sect. 3.3) displays significant amounts of the high-affinity Man6 (75%) and Man5 (8%) receptors [127].

Steered molecular dynamics simulations predicted that application of tensile force along the long axis of FimH (as might result, e.g. from shear forces) would result in extension of the linker region between the receptor-binding and pilin domains [163]. As mentioned above, extension of the linker was proposed to facilitate the formation of catch bonds. Congruent with this idea, bacteria expressing type 1 fimbriae with either naturally occurring or engineered FimH variants with mutations predicted to destabilize the linker region and facilitate linker extension were shown to exhibit decreased shear-dependent adhesion. Recently, a two-state catch-bond model derived from allostery that beautifully explains and predicts the data observed for stick-and-roll adhesion of type 1 fimbriated *E. coli* to mannose-coated surfaces was proposed [181]. In contrast to the sliding-rebinding mechanism proposed for catch-bond formation in P and L selectins [184], this model involves two interchangeable conformational states of the mannose-binding pocket. Extension of the FimH linker is proposed to allosterically change the binding pocket from a weak to a tight-binding conformation. The crystal structures of mannose and of butyl-mannose bound to FimH [57, 147] show that mannose binds snugly into a highly specific mannose-binding pocket at the tip of the FimH receptor-binding domain (see Sect. 3.4). As indicated by the unusually high monosaccharide affinity of FimH for mannose (K_d = 2.3 μM), the pocket appears near-optimal for mannose binding with almost all of the hydrogen-bonding potential satisfied. Hence it is difficult to envision how conformational changes could additionally enhance mannose binding. It is possible that the observed structures correspond to the tight-binding conformation, and that the weak-binding conformation is not favoured by the crystallization conditions used to grow crystals. In this context it is worth noting that automated docking studies of mannose binding to FimH predicts two main binding modes, one corresponding to that observed in the crystal structures, and a second binding mode in which the mannose residue is rotated within the binding pocket (J. Berglund, D. Choudhury, S.D. Knight, unpublished).

3.6 Medical Applications

3.6.1 Vaccines

Vaccines targeting some bacterial infections (e.g. pertussis, typhoid fever, ETEC diarrhoea and bovine mastitis, e.g. [185–187], and glycoconjugate vaccines targeting *Haemophilus*, *Neisseria* and *Streptococcus*, e.g. [188–190]) are available or are being developed. With the exception of the highly successful glycoconjugate vaccines, many vaccines have been formulated using either killed whole bacteria or live attenuated bacterial strains. Such whole cell vaccines are associated with a number of problems such as more or less severe side effects (severe local reactions, fever), the need for rigorous safety measures to ensure that live pathogenic bacteria are not spread from the production plant or transferred with the vaccine, or problems of controlling the stability, strength, and nature of immune response owing to variations in

antigen presentation and in the amount of antigen present in the vaccine. Additionally, whole cell antigen presentation may shield potentially efficient broad-range antigens from the immune system. This is the case with TDA fimbriae, where a conserved (e.g. [57]) and intrinsically highly antigenic receptor-binding adhesin is incorporated as a minor component of a large complex protein structure on the bacterial cell surface, leading to efficient production of antibodies directed against the much less conserved bulk components of the organelle but not against the adhesin.

Because of their critical role in pathogenesis and because they are naturally expressed on the surface of bacteria, bacterial adhesins have long been considered as attractive components of vaccines [191], so far with only limited success. Many adhesin vaccine formulations have been based on intact adhesive organelles (e.g. fimbriae), which are antigenically highly variable and hence induce protection limited to bacteria expressing the same fimbrial variant. For example, antibodies directed against purified whole type 1 fimbriae or P pili protect against cystitis and pyelonephritis respectively, in both murine and primate models for these diseases [14, 17, 192–194]. However, protection is limited to either *E. coli* strains homologous to that from which the fimbriae used for immunization were derived, or to a small subset of serologically cross-reactive heterologous strains. Therefore, any vaccine composed predominantly of the major structural proteins of fimbriae (e.g. FimA or PapA) will be of limited value because antibodies developed against these highly variable proteins are specific for the strains from which the protein used for immunization was derived.

The realization that TDAs could be obtained as stable and soluble complexes with their cognate chaperone inspired new hope for the development of adhesin-based vaccines. Promising preclinical trials with UTI vaccines based on the FimC:FimH chaperone:adhesin complex [195] and on the PapD:PapG chaperone:adhesin complex [21, 196] have been reported. Both vaccine candidates were shown to protect against UPEC mucosal infection in murine and primate models. In vitro binding data suggested that the ability of anti-FimH antibodies to block type 1 fimbrial adhesion contributed significantly to FimC:FimH-induced protection. No clinical trials with the PapD:PapG vaccine have as of yet been reported. Development of the FimC:FimH vaccine candidate was dropped during phase II clinical trials because of limited protection (MedImmune, Inc., Annual Report 2002).

One possible reason for the limited success with adhesin subunit vaccines might relate to how these vaccines have been formulated. Monomeric presentation of antigens such as that used for the FimC:FimH and PapD:PapG UTI vaccines often gives poor immunogenic response. Multivalent antigen presentation generally results in a significantly improved response [197]. Multivalent antigen presentation may be achieved by coupling subunit antigens to a suitable carrier particle. For multivalent presentation to be efficient, antigens must be coupled without disturbing their antigenic capacity. Ideally, antigens should be presented on the carrier particle in the same way as they would be on the surface of the pathogen from which they have been derived, so as to present the immune system with a good mimic of the pathogen surface. In the case of adhesins, the receptor binding function must not be destroyed, or masked, if blocking antibodies are to be raised. Several recent examples show that the receptor-binding domain of TDAs such as

FimH or PapG may be expressed on its own without affecting the structure or binding properties [142, 143, 147, 198–200]. Since the carbohydrate binding site is located in the top half of the receptor-binding domains, distal from the C-terminal linker region that connects it to the pilin domain in the full length TDAs, modified proteins consisting of the isolated receptor-binding domain coupled to a suitable C-terminal tag could be used to incorporate functional adhesins into multivalent antigen-carrying particles for use as vaccines. Using this approach, we recently produced FimH-decorated ISCOM [197, 201, 202] particles, and are investigating the immunogenic properties of these particles (G. Askarieh, J.-I. Flock, S.D. Knight, unpublished).

3.6.2 Pilicides

Pilicides are small organic molecules designed to interfere with pilus biogenesis [203, 204]. The activity of a family of bicyclic 2-pyridones, termed pilicides, has been evaluated in two different UPEC fimbrial systems, and its interactions have been examined in detail in a crystal structure of the FimC:FimH chaperone-adhesin complex with a bound pilicide [205]. The binding of the pilicide would interfere with the binding of the N-terminal periplasmic domain of the usher to the chaperone-pilin interface, particularly of the bulky hydrophobic usher residues Phe4, Leu19, and Phe22 [68]. Note that this was an unexpected result since the pilicide had been designed to bind to the chaperone cleft and block subunit binding.

3.6.3 Anti-Adhesives

An alternative to adhesin-based vaccines as a means to block bacterial adhesion is the use of small compounds that interact tightly with target adhesins [206]. Aromatically substituted mannosides have long been known to be particularly potent inhibitors (nanomolar binding constants) of FimH-mediated bacterial adhesion [207]. Fruit juice, in particular cranberry juice [208], has traditionally been considered to be useful in the treatment of UTIs, and a positive effect of cranberry juice consumption has been observed in controlled clinical trials (e.g. [209–211]). Fructose has been shown to be the active compound in fruit juices that inhibits adhesion of type 1 fimbriated *E. coli* [208]. Fructose binding to FimH is only ~15 times weaker than mannose binding, and fructose binds more tightly to FimH than the physiological P pilus globotetraoside receptor does to PapG-II [147].

We recently reported two independent crystal structures for the FimH receptor-binding domain [147]. In both structures we found a butyl mannoside, derived from the yeast extract used to grow bacteria for protein expression, bound in the mannose-binding site. The serendipitous discovery of this ‘sticky’ ligand led to the identification of alkyl mannosides as a new class of high-affinity FimH ligands. The mannose group of the butyl mannoside binds identically to D-mannose (Fig. 9c). The alkyl chain extends out of the pocket towards Tyr48 and Tyr137, making van

der Waals contacts to both tyrosine rings. We discovered that butyl α-D-mannoside binds to FimH significantly better (K_d ~150 nM) than mannose (K_d ~2.3 μM). To investigate the effect of sequential addition of methyl groups to the O1 oxygen of D-mannose, a series of alkyl mannosides were synthesized and the dissociation constants determined using two different binding assays. We discovered a linear correlation between the binding free energy, as calculated from the measured dissociation constants, and the number of methyl groups (between 1 and 7) in the alkyl mannoside, with each additional methyl group contributing on average –0.6 kcal mol^{-1} of binding energy. The best binding alkyl mannoside, heptyl mannoside, binds a few hundred times stronger than mannose, equivalent in affinity to the most tightly-binding aromatically substituted mannosides for FimH and of mannose dendrimers for type 1 fimbriated *E. coli* [207, 212]. Alkyl mannosides have not previously been recognized as strong binders to FimH. Since they are easily synthesized and highly soluble in water, they may be interesting as potential blocking agents for FimH-mediated adhesion.

Just as polyvalent binding is used by bacteria to enhance adhesion, polyvalency can potentially be used to create potent adhesion inhibitors. Because small molecule adhesin inhibitors with sufficient affinity to block bacterial adhesion might be hard to accomplish, a lot of interest lies in the design of multivalent anti-adhesives that target several fimbrial adhesins simultaneously. However, the design of multivalent inhibitors for fimbrial adhesins is much more complicated than for multimeric multivalent proteins. For the latter, a relatively constant distance between the binding sites can be predicted, depending on the quaternary organization of the multimeric protein. For fimbriated bacteria on the other hand, the spacing between the fimbrial adhesins is not constant and difficult to estimate. The length of type 1 fimbriae can vary considerably. Also the number of fimbriae expressed on the cell envelope and hence the average spacing between them can vary between strains and moreover depends on the growth conditions favouring or disfavouring expression. Because type 1 and P fimbrial expression are known to be subject to phase regulation (see Sect. 3.1), normally only a percentage of *E. coli* cells in a population are fimbriated. The fimbrial tip, including the FimH adhesin, may break off under shear force for example during preparation steps prior to the analysis of the bacterial cells, making it difficult to asses the number of functional fimbriae present. Finally, although type 1 fimbriae are relatively rigid, their extended shape allows them some freedom to wave around in the solvent. The short, stubby tip fibrillum is flexible. All of these factors increase the uncertainty in distances between the targeted FimH receptor-binding domains making both the design process and evaluation of results more difficult.

The plasticity of the fimbrial rod and the flexibility of the tip fibrillum help to increase the number of possible encounters of the fimbrial adhesins with the sugar epitopes on the host cells. In this regard, the distance between the sugar receptors on a surface to be bridged by the fimbrial adhesins is not fixed and does not really have a strict upper limit. A minimal distance between two mannose epitopes can however easily be imagined, as two FimH receptor-binding domains on two fimbriae cannot be brought together too closely. A first idea of a minimal

distance between two sugar epitopes can be obtained by considering binding of alkyl mannosides to the mannose-binding site of FimH. The length of an alkyl tail O-linked to α-D-mannose that is optimal for interaction with FimH is seven carbon atoms (K_d = 5 nM for heptyl α-D-mannose) [147]. This suggests that a linker between two mannose residues that are both meant for interaction with FimH theoretically should be at least 14–16 atoms long for the two binding surfaces of FimH not to sterically interfere with each other. The enhanced binding of alkyl and aryl mannosides demonstrates that the first part of the aglycon in a polyvalent mannose compound should in fact not even be considered as a linker, but as part of the ligand.

Type 1 fimbriated UPEC have probably been the most extensively studied target of glycodendrimer chemistry [212, 213]. Nevertheless, glycodendrimer chemistry designed to inhibit type 1 mediated bacterial adherence has proven excruciatingly difficult. The most successful example of a large glycodendrimer FimH inhibitor is the DP16 dendrimer designed by Nagahori et al. [212]. This inhibitor inhibits type 1 fimbrial adhesion considerably better (sub-nanomolar IC_{50} values) than monovalent mannose but still not significantly better than the best-known small-molecule inhibitors. The difficulties in finding strong multivalent adhesion inhibitors could be solely due to incorrect linkage of the mannose residue in the dendrimer, preventing mannose from binding in the mannose binding pocket of FimH [214], but most often reflects the difficulties in trying to use molecular ligands to simulate the complexity of multivalent cellular host-pathogen interactions.

4 Conclusion and Perspectives

During the last decade, considerable progress has been made in understanding chaperone/usher-mediated fimbrial assembly, and the contribution of fimbriae to bacterial adhesion and disease. By providing a folding platform consisting of a pair of template β-strands (A_1 and G_1), and large hydrophobic donor residues, periplasmic chaperones promote subunit folding and partition intrinsically aggregative protein subunits away from non-productive aggregation pathways. Subunit folding onto this platform results in chaperone donor residues being incorporated into the core of the subunit and formation of a fused super-barrel with the subunit in an open, activated high-energy conformation. Following dissociation of this activated subunit from the chaperone, folding is completed to form a condensed hydrophobic core. By arresting subunit folding and trapping subunits in a molten globule-like high-energy conformation, the chaperones preserve folding energy that can drive assembly even when chaperone:subunit interactions are more extensive than subunit:subunit interactions in the fibre. In contrast to the rather detailed understanding of the periplasmic chaperones, very little is still known about the assembly process per se and the workings of the outer membrane usher. A first glimpse of how the usher recognizes chaperone:subunit complexes has provided some hints about how specificity and ordered assembly of complex structures is achieved. In the following years,

hopefully new structures of ushers, and of complexes between ushers and chaperones and subunits will allow us to begin to fill in the remaining gaps in our understanding of fimbrial assembly. Understanding the molecular details of fimbrial biogenesis will continue to contribute to our ability to invent and/or discover new agents that interfere with the process (exemplified by the recent success with pilicides) and that may become useful in the treatment of bacterial infections.

Our understanding of bacterial adhesion has now reached a level where we can begin to exploit it for the development of novel anti-adhesive compounds for use in, e.g. medicine. Structural insight into the host-pathogen fimbrial interactions can significantly facilitate rational design of highly potent, small, and monovalent sugar-derived inhibitors that are relatively easy to synthesize; and finally truly polyvalent, dendrimeric inhibitors could be derived from these. Other future anti-adhesive therapies will focus on the cellular biology of the bacterial attachment, invasion, and reproduction processes. A first step in that direction has been made by the treatment of mouse bladder with an exfoliation agent, protamine sulphate, to remove cells containing bacterial reproduction factories from the superficial endothelial cell barrier of the bladder [215].

Acknowledgements We thank Anton Zavialov for careful reading of the manuscript and critical comments. Financial support from the Swedish Research Council to SDK and from the Fonds voor Wetenschappelijk Onderzoek – Vlaanderen (FWO) to JB is gratefully acknowledged.

References

1. WHO (2004) World Health Report 2004: changing history. World Health Organization, Geneva
2. Osrin D, Vergnano S, Costello A (2004) *Curr Opin Infect Dis* 17:217
3. Nordberg P, Monnet DL, Cars O (2005) WHO Department of Medicines Policy and Standards
4. White DG, McDermott PF (2001) *J Dairy Sci* 84(E Suppl):E151
5. Roumagnac P, Weill XF, Dolecek C, Baker S, Brisse S, Nguyen TC, Hong Le TA, Acosta CJ, Farrar J, Dougan G, Achtman M (2006) *Science* 314:1301
6. Gupta K (2003) *Infect Dis Clin North Am* 17:243
7. Stamm WE, Hooton TM (1993) *N Engl J Med* 329:1328
8. Ronald A (2002) *Am J Med* 113:14S
9. Berglund J, Knight SD (2003) *Adv Exp Med Biol* 535:33
10. Mulvey MA (2002) *Cell Microbiol* 4:257
11. Soto GE, Hultgren SJ (1999) *J Bacteriol* 181:1059
12. Connell H, Agace W, Klemm P, Schembri M, Marild S, Svanborg C (1996) *Proc Natl Acad Sci USA* 93:9827
13. Thankavel K, Madison B, Ikeda T, Malaviya R, Shah AH, Arumugam PM, Abraham SN (1997) *J Clin Invest* 100:1123
14. Langermann S, Palaszynski S, Barnhart M, Auguste G, Pinkner JS, Burlein J, Barren P, Koenig S, Leath S, Jones CH, Hultgren SJ (1997) *Science* 276:607
15. Mulvey MA, Lopez-Boado YS, Wilson CL, Roth R, Parks WC, Heuser J, Hultgren SJ (1998) *Science* 282:1494

16. Bahrani-Mougeot FK, Buckles EL, Lockatell CV, Hebel JR, Johnson DE, Tang CM, Donnenberg MS (2002) *Mol Microbiol* 45:1079
17. Roberts JA, Marklund BI, Ilver D, Haslam D, Kaack MB, Baskin G, Louis M, Mollby R, Winberg J, Normark S (1994) *Proc Natl Acad Sci USA* 91:11889
18. Langermann S, Ballou WR Jr (2001) *J Infect Dis 183 Suppl* 1:S84
19. Langermann S, Mollby R, Burlein JE, Palaszynski SR, Auguste CG, DeFusco A, Strouse R, Schenerman MA, Hultgren SJ, Pinkner JS, Winberg J, Guldevall L, Soderhall M, Ishikawa K, Normark S, Koenig S (2000) *J Infect Dis* 181:774
20. Pecha B, Low D, O'Hanley P (1989) *J Clin Invest* 83:2102
21. Roberts JA, Kaack MB, Baskin G, Chapman MR, Hunstad DA, Pinkner JS, Hultgren SJ (2004) *J Urol* 171:1682
22. Duguid JP, Anderson ES (1967) *Nature* 215:89
23. van Driessche E, Schoup J, Charlier G, Lintermans P, Beeckmans S, Zeeuws R, Pohl P, Kanarek L (1988) In: Bøg-Hansen TC, Freed DLJ (eds) Lectins: biology, biochemistry, clinical biochemistry. Proceedings of the 9th International Lectin Meeting in Cambridge in 1987, vol 6. Sigma Chemical Company, St Louis, USA, p 55
24. Chen TH, Elberg SS (1977) *Infect Immun* 15:972
25. Hung DL, Knight SD, Woods RM, Pinkner JS, Hultgren SJ (1996) *EMBO J* 15:3792
26. Thanassi DG, Saulino ET, Hultgren SJ (1998) *Curr Opin Microbiol* 1:223
27. Hung DL, Hultgren SJ (1998) *J Struct Biol* 124:201
28. Knight SD, Berglund J, Choudhury D (2000) *Curr Opin Chem Biol* 4:653
29. Sauer FG, Barnhart M, Choudhury D, Knight SD, Waksman G, Hultgren SJ (2000) *Curr Opin Struct Biol* 10:548
30. Sauer FG, Remaut H, Hultgren SJ, Waksman G (2004) *Biochim Biophys Acta* 1694:259
31. Capitani G, Eidam O, Glockshuber R, Grutter MG (2006) *Microbes Infect* 8:2284
32. Choudhury D, Thompson A, Stojanoff V, Langermann S, Pinkner J, Hultgren SJ, Knight SD (1999) *Science* 285:1061
33. Sauer FG, Futterer K, Pinkner JS, Dodson KW, Hultgren SJ, Waksman G (1999) *Science* 285:1058
34. Sauer FG, Pinkner JS, Waksman G, Hultgren SJ (2002) *Cell* 111:543
35. Zavialov AV, Berglund J, Pudney AF, Fooks LJ, Ibrahim TM, MacIntyre S, Knight SD (2003) *Cell* 113:587
36. Jedrzejczak R, Dauter Z, Dauter M, Piatek R, Zalewska B, Mroz M, Bury K, Nowicki B, Kur J (2006) *Acta Crystallogr D Biol Crystallogr* 62:157
37. Korotkova N, Le Trong I, Samudrala R, Korotkov K, Van Loy CP, Bui AL, Moseley SL, Stenkamp RE (2006) *J Biol Chem* 281:22367
38. Pettigrew D, Anderson KL, Billington J, Cota E, Simpson P, Urvil P, Rabuzin F, Roversi P, Nowicki B, du Merle L, Le Bouguenec C, Matthews S, Lea SM (2004) *J Biol Chem* 279:46851
39. Remaut H, Rose RJ, Hannan TJ, Hultgren SJ, Radford SE, Ashcroft AE, Waksman G (2006) *Mol Cell* 22:831
40. Verger D, Miller E, Remaut H, Waksman G, Hultgren S (2006) *EMBO Rep* 7:1228
41. Zavialov AV, Tischenko VM, Fooks LJ, Brandsdal BO, Aqvist J, Zav'yalov VP, Macintyre S, Knight SD (2005) *Biochem J* 389:685
42. Soto GE, Dodson KW, Ogg D, Liu C, Heuser J, Knight S, Kihlberg J, Jones CH, Hultgren SJ (1998) *EMBO J* 17:6155
43. Zavialov AV, Kersley J, Korpela T, Zav'yalov VP, MacIntyre S, Knight SD (2002) *Mol Microbiol* 45:983
44. Piatek R, Zalewska B, Kolaj O, Ferens M, Nowicki B, Kur J (2005) *Infect Immun* 73:135
45. Krogfelt KA, Bergmans H, Klemm P (1990) *Infect Immun* 58:1995
46. Jones CH, Pinkner JS, Roth R, Heuser J, Nicholes AV, Abraham SN, Hultgren SJ (1995) *Proc Natl Acad Sci USA* 92:2081
47. Hahn E, Wild P, Hermanns U, Sebbel P, Glockshuber R, Haner M, Taschner N, Burkhard P, Aebi U, Muller SA (2002) *J Mol Biol* 323:845

48. Makhatadze GI, Privalov PL (1995) *Adv Protein Chem* 47:307
49. Meersman F, Smeller L, Heremans K (2006) *Biochim Biophys Acta* 1764:346
50. Stathopoulos C, Hendrixson DR, Thanassi DG, Hultgren SJ, St Geme JW III , Curtiss R III (2000) *Microbes Infect* 2:1061
51. Munera D, Hultgren S, Fernández LA (2007) Mol Microbiol (OnlineAccepted Articles): doi:10.1111/j.1365
52. So SS, Thanassi DG (2006) *Mol Microbiol* 60:364
53. Saulino ET, Thanassi DG, Pinkner JS, Hultgren SJ (1998) *EMBO J* 17:2177
54. Saulino ET, Bullitt E, Hultgren SJ (2000) *Proc Natl Acad Sci USA* 97:9240
55. Vetsch M, Sebbel P, Glockshuber R (2002) *J Mol Biol* 322:827
56. Jacob-Dubuisson F, Striker R, Hultgren SJ (1994) *J Biol Chem* 269:12447
57. Hung CS, Bouckaert J, Hung D, Pinkner J, Widberg C, DeFusco A, Auguste CG, Strouse R, Langermann S, Waksman G, Hultgren SJ (2002) *Mol Microbiol* 44:903
58. Kuehn MJ, Ogg DJ, Kihlberg J, Slonim LN, Flemmer K, Bergfors T, Hultgren SJ (1993) *Science* 262:1234
59. Slonim LN, Pinkner JS, Branden CI, Hultgren SJ (1992) *EMBO J* 11:4747
60. Vetsch M, Erilov D, Moliere N, Nishiyama M, Ignatov O, Glockshuber R (2006) *EMBO Rep* 7:734
61. Vetsch M, Puorger C, Spirig T, Grauschopf U, Weber-Ban EU, Glockshuber R (2004) *Nature* 431:329
62. Henderson NS, So SS, Martin C, Kulkarni R, Thanassi DG (2004) *J Biol Chem* 279:53747
63. Nishiyama M, Vetsch M, Puorger C, Jelesarov I, Glockshuber R (2003) *J Mol Biol* 330:513
64. Thanassi DG, Stathopoulos C, Dodson K, Geiger D, Hultgren SJ (2002) *J Bacteriol* 184:6260
65. Li H, Qian L, Chen Z, Thibault D, Liu G, Liu T, Thanassi DG (2004) *J Mol Biol* 344:1397
66. Barnhart MM, Sauer FG, Pinkner JS, Hultgren SJ (2003) *J Bacteriol* 185:2723
67. Ng TW, Akman L, Osisami M, Thanassi DG (2004) *J Bacteriol* 186:5321
68. Nishiyama M, Horst R, Eidam O, Herrmann T, Ignatov O, Vetsch M, Bettendorff P, Jelesarov I, Grutter MG, Wuthrich K, Glockshuber R, Capitani G (2005) *EMBO J* 24:2075
69. Capitani G, Eidam O, Grutter MG (2006) *Proteins* 65:816
70. Duguid JP, Anderson ES, Campbell I (1966) *J Pathol Bacteriol* 92:107
71. Brinton CC Jr (1965) *Trans N Y Acad Sci* 27:1003
72. Boyd EF, Hartl DL (1999) *J Bacteriol* 181:1301
73. Kulasekara HD, Blomfield IC (1999) *Mol Microbiol* 31:1171
74. Valenski ML, Harris SL, Spears PA, Horton JR, Orndorff PE (2003) *J Bacteriol* 185:5007
75. Rossolini GM, Muscas P, Chiesurin A, Satta G (1993) *FEMS Microbiol Lett* 114:259
76. Chu D, Blomfield IC (2007) *J Theor Biol* 244:541
77. Abraham JM, Freitag CS, Clements JR, Eisenstein BI (1985) *Proc Natl Acad Sci USA* 82:5724
78. Gally DL, Leathart J, Blomfield IC (1996) *Mol Microbiol* 21:725
79. Klemm P (1986) *EMBO J* 5:1389
80. McClain MS, Blomfield IC, Eisenstein BI (1991) *J Bacteriol* 173:5308
81. Welch RA, Burland V, Plunkett G III, Redford P, Roesch P, Rasko D, Buckles EL, Liou SR, Boutin A, Hackett J, Stroud D, Mayhew GF, Rose DJ, Zhou S, Schwartz DC, Perna NT, Mobley HL, Donnenberg MS, Blattner FR (2002) *Proc Natl Acad Sci USA* 99:17020
82. Bryan A, Roesch P, Davis L, Moritz R, Pellett S, Welch RA (2006) *Infect Immun* 74:1072
83. Xie Y, Yao Y, Kolisnychenko V, Teng CH, Kim KS (2006) *Infect Immun* 74:4039
84. Blomfield IC, Kulasekara DH, Eisenstein BI (1997) *Mol Microbiol* 23:705
85. Gally DL, Rucker TJ, Blomfield IC (1994) *J Bacteriol* 176:5665
86. Roesch Rl, Blomfield IC (1998) *Mol Microbiol* 27:751
87. Olsen PB, Schembri MA, Gally DL, Klemm P (1998) *FEMS Microbiol Lett* 162:17
88. El-Labany S, Sohanpal BK, Lahooti M, Akerman R, Blomfield IC (2003) *Mol Microbiol* 49:1109
89. Sohanpal BK, El Labany S, Lahooti M, Plumbridge JA, Blomfield IC (2004) *Proc Natl Acad Sci USA* 101:16322

90. Sohanpal BK, Friar S, Roobol J, Plumbridge JA, Blomfield IC (2007) *Mol Microbiol* 63:1223
91. Blumer C, Kleefeld A, Lehnen D, Heintz M, Dobrindt U, Nagy G, Michaelis K, Emody L, Polen T, Rachel R, Wendisch VF, Unden G (2005) *Microbiology* 151:3287
92. Schwan WR, Beck MT, Hultgren SJ, Pinkner J, Woolever NL, Larson T (2005) *Infect Immun* 73:1226
93. Snyder JA, Lloyd AL, Lockatell CV, Johnson DE, Mobley HL (2006) *Infect Immun* 74:1387
94. Holden NJ, Totsika M, Mahler E, Roe AJ, Catherwood K, Lindner K, Dobrindt U, Gally DL (2006) *Microbiology* 152:1143
95. Xia Y, Gally D, Forsman-Semb K, Uhlin BE (2000) *EMBO J* 19:1450
96. Snyder JA, Haugen BJ, Lockatell CV, Maroncle N, Hagan EC, Johnson DE, Welch RA, Mobley HLT (2005) *Infect Immun* 73:7588
97. Holden NJ, Gally DL (2004) *J Med Microbiol* 53:585
98. Kau AL, Hunstad DA, Hultgren SJ (2005) *Curr Opin Microbiol* 8:54
99. Teng CH, Cai M, Shin S, Xie Y, Kim KJ, Khan NA, Di Cello F, Kim KS (2005) *Infect Immun* 73:2923
100. Barnich N, Boudeau J, Claret L, Darfeuille-Michaud A (2003) *Mol Microbiol* 48:781
101. Boudeau J, Barnich N, Darfeuille-Michaud A (2001) *Mol Microbiol* 39:1272
102. Vandemaele FJ, Hensen SM, Goddeeris BM (2004) *Vet Microbiol* 101:147
103. Dopfer D, Almeida RA, Lam TJ, Nederbragt H, Oliver SP, Gaastra W (2000) *Vet Microbiol* 74:331
104. Dopfer D, Nederbragt H, Almeida RA, Gaastra W (2001) *Vet Microbiol* 80:285
105. Lammers A, van Vorstenbosch CJ, Erkens JH, Smith HE (2001) *Vet Microbiol* 80:255
106. Bradley AJ, Green MJ (2001) *J Clin Microbiol* 39:1845
107. Feria C, Machado J, Correia JD, Goncalves J, Gaastra W (2001) *Vet Microbiol* 82:81
108. Mulvey MS, Lopez-Boado YS, Wilson CL, Roth R, Parks WC, Heuser J, Hultgren SJ (1998) *Science* 282:1494
109. Fischer H, Yamamoto M, Akira S, Beutler B, Svanborg C (2006) *Eur J Immunol* 36:267
110. Samuelsson P, Hang L, Wullt B, Irjala H, Svanborg C (2004) *Infect Immun* 72:3179
111. Schilling JD, Martin SM, Hunstad DA, Patel KP, Mulvey MA, Justice SS, Lorenz RG, Hultgren SJ (2003) *Infect Immun* 71:1470
112. Russo TA, Stapleton A, Wenderoth S, Hooton TM, Stamm WE (1995) *J Infect Dis* 172:440
113. Wright KJ, Hultgren SJ (2006) *Future Microbiol* 1:75
114. Anderson GG, Palermo JJ, Schilling JD, Roth R, Heuser J, Hultgren SJ (2003) *Science* 301:105
115. Garofalo CK, Hooton TM, Martin SM, Stamm WE, Palermo JJ, Gordon JI, Hultgren SJ (2007) *Infect Immun* 75:52
116. Justice SS, Hung C, Theriot JA, Fletcher DA, Anderson GG, Footer MJ, Hultgren SJ (2004) *Proc Natl Acad Sci USA* 101:1333
117. Schilling JD, Hultgren SJ (2002) *Int J Antimicrob Agents* 19:457
118. Justice SS, Lauer SR, Hultgren SJ, Hunstad DA (2006) *Infect Immun* 74:4793
119. Pratt LA, Kolter R (1998) *Mol Microbiol* 30:285
120. Donlan RM, Costerton JW (2002) *Clin Microbiol Rev* 15:167
121. Schembri MA, Givskov M, Klemm P (2002) *Sci STKE* 2002:re6
122. Van Houdt R, Michiels CW (2005) *Res Microbiol* 156:626
123. Orndorff PE, Devapali A, Palestrant S, Wyse A, Everett ML, Bollinger RR, Parker W (2004) *Infect Immun* 72:1929
124. Hasman H, Chakraborty T, Klemm P (1999) *J Bacteriol* 181:4834
125. Danese PN, Pratt LA, Dove SL, Kolter R (2000) *Mol Microbiol* 37:424
126. Schembri MA, Klemm P (2001) *EMBO J* 20:3074
127. Cavallone D, Malagolini N, Monti A, Wu XR, Serafini-Cessi F (2004) *J Biol Chem* 279:216
128. Wu XR, Sun TT, Medina JJ (1996) *Proc Natl Acad Sci USA* 93:9630

129. Zhou G, Mo WJ, Sebbel P, Min G, Neubert TA, Glockshuber R, Wu XR, Sun TT, Kong XP (2001) *J Cell Sci* 114:4095
130. Wu XR, Medina JJ, Sun TT (1995) *J Biol Chem* 270:29752
131. Yu J, Lin JH, Wu XR, Sun TT (1994) *J Cell Biol* 125:171
132. Min G, Stolz M, Zhou G, Liang F, Sebbel P, Stoffler D, Glockshuber R, Sun TT, Aebi U, Kong XP (2002) *J Mol Biol* 317:697
133. Xie B, Zhou G, Chan SY, Shapiro E, Kong XP, Wu XR, Sun TT, Costello CE (2006) *J Biol Chem* 281:14644
134. Dimri GP, Lee XH, Basile G, Acosta M, Scott C, Roskelley C, Medrano EE, Linskens M, Rubelj I, Pereirasmith O, Peacocke M, Campisi J (1995) *Proc Natl Acad Sci USA* 92:9363
135. Daher A, de Boer WI, Le Frere-Belda MA, Kheuang L, Abbou CC, Radvanyi F, Jaurand MC, Thiery JP, Gil Diez De Medina S, Chopin DK (2004) *Eur Urol* 45:799
136. Jost SP (1989) *Virchows Arch B Cell Path Inc Mol Path* 57:27
137. Pak J, Pu Y, Zhang ZT, Hasty DL, Wu XR (2001) *J Biol Chem* 276:9924
138. Bates JM, Raffi HM, Prasadan K, Mascarenhas R, Laszik Z, Maeda N, Hultgren SJ, Kumar S (2004) *Kidney Int* 65:791
139. Mo L, Zhu XH, Huang HY, Shapiro E, Hasty DL, Wu XR (2004) *Am J Physiol Renal Physiol* 286:F795
140. van Rooijen JJM, Voskamp AF, Kamerling JP, Vliegenthart JFG (1999) *Glycobiology* 9:21
141. Bouckaert J, Mackenzie J, de Paz JL, Chipwaza B, Choudhury D, Zavialov A, Mannerstedt K, Anderson J, Pierard D, Wyns L, Seeberger PH, Oscarson S, De Greve H, Knight SD (2006) *Mol Microbiol* 61:1556
142. Dodson KW, Pinkner JS, Rose T, Magnusson G, Hultgren SJ, Waksman G (2001) *Cell* 105:733
143. Buts L, Bouckaert J, De Genst E, Loris R, Oscarson S, Lahmann M, Messens J, Brosens E, Wyns L, De Greve H (2003) *Mol Microbiol* 49:705
144. Anderson KL, Billington J, Pettigrew D, Cota E, Simpson P, Roversi P, Chen HA, Urvil P, du Merle L, Barlow PN, Medof ME, Smith RA, Nowicki B, Le Bouguenec C, Lea SM, Matthews S (2004) *Mol Cell* 15:647
145. Cota E, Jones C, Simpson P, Altroff H, Anderson KL, du Merle L, Guignot J, Servin A, Le Bouguénec C, Mardon H, Matthews S (2006) *Mol Microbiol* 62:356
146. Bork P, Holm L, Sander C (1994) *J Mol Biol* 242:309
147. Bouckaert J, Berglund J, Schembri M, De Genst E, Cools L, Wuhrer M, Hung CS, Pinkner J, Slattegard R, Zavialov A, Choudhury D, Langermann S, Hultgren SJ, Wyns L, Klemm P, Oscarson S, Knight SD, De Greve H (2005) *Mol Microbiol* 55:441
148. Nicholls A, Sharp KA, Honig B (1991) *Proteins* 11:281
149. Firon N, Ofek I, Sharon N (1983) *Carbohydr Res* 120:235
150. Firon N, Ofek I, Sharon N (1984) *Infect Immun* 43:1088
151. Sharon N, Firon N, Ofek I (1983) *Pure Appl Chem* 55:671
152. Neeser J-R, Koellreutter B, Wuersch P (1986) *Infect Immun* 52:428
153. Rockendorf N, Sperling O, Lindhorst TK (2002) *Austr J Chem* 55:87
154. Loris R, Tielker D, Jaeger KE, Wyns L (2003) *J Mol Biol* 331:861
155. Loris R, Imberty A, Beeckmans S, Van Driessche E, Read JS, Bouckaert J, De Greve H, Buts L, Wyns L (2003) *J Biol Chem* 278:16297
156. Calarese DA, Scanlan CN, Zwick MB, Deechongkit S, Mimura Y, Kunert R, Zhu P, Wormald MR, Stanfield RL, Roux KH, Kelly JW, Rudd PM, Dwek RA, Katinger H, Burton DR, Wilson IA (2003) *Science* 300:2065
157. Firon N, Ofek I, Sharon N (1982) *Biochem Biophys Res Commun* 105:1426
158. Rosenstein IJ, Stoll MS, Mizuochi T, Childs RA, Hounsell EF, Feizi T (1988) *Lancet* 2:1327
159. Durand G, Seta N (2000) *Clin Chem* 46:795
160. Hoepelman AIM, Meiland R, Geerlings SE (2003) *Int J Antimicrob Agents* 22:S35
161. Geerlings SE, Meiland R, van Lith EC, Brouwer EC, Gaastra W, Hoepelman AI (2002) *Diabetes Care* 25:1405

162. Sokurenko EV, Chesnokova V, Doyle RJ, Hasty DL (1997) *J Biol Chem* 272:17880
163. Thomas WE, Trintchina E, Forero M, Vogel V, Sokurenko EV (2002) *Cell* 109:913
164. Sokurenko EV, Chesnokova V, Dykhuizen DE, Ofek I, Wu XR, Krogfelt KA, Struve C, Schembri MA, Hasty DL (1998) *Proc Natl Acad Sci USA* 95:8922
165. Sokurenko EV, Courtney HS, Maslow J, Siitonen A, Hasty DL (1995) *J Bacteriol* 177:3680
166. Sokurenko EV, Courtney HS, Ohman DE, Klemm P, Hasty DL (1994) *J Bacteriol* 176:748
167. Beskhlebnaya VA, Trinchina EV, Aprikyan P, Chesnokova V, Sokurenko EV (2006) *Bull Exp Biol Med* 141:339
168. Liang MN, Smith SP, Metallo SJ, Choi IS, Prentiss M, Whitesides GM (2000) *Proc Natl Acad Sci USA* 97:13092
169. Madison B, Ofek I, Clegg S, Abraham SN (1994) *Infect Immun* 62:843
170. Thankavel K, Shah AH, Cohen MS, Ikeda T, Lorenz RG, Curtiss R III, Abraham SN (1999) *J Biol Chem* 274:5797
171. Duncan MJ, Mann EL, Cohen MS, Ofek I, Sharon N, Abraham SN (2005) *J Biol Chem* 280:37707
172. Gong M, Makowski L (1992) *J Mol Biol* 228:735
173. Abraham SN, Land M, Ponniah S, Endres R, Hasty DL, Babu JP (1992) *J Bacteriol* 174:5145
174. Bullitt E, Makowski L (1995) *Nature* 373:164
175. Fallman E, Schedin S, Jass J, Uhlin BE, Axner O (2005) *EMBO Reports* 6:52
176. Miller E, Garcia TI, Hultgren S, Oberhauser A (2006) *Biophys J* 91:3848
177. Forero M, Yakovenko O, Sokurenko EV, Thomas WE, Vogel V (2006) *PLoS Biology* 4:1509
178. Anderson BN, Ding AM, Nilsson LM, Kusuma K, Tchesnokova V, Vogel V, Sokurenko EV, Thomas WE (2007) *J Bacteriol* 189:1794
179. Nilsson LM, Thomas WE, Sokurenko EV, Vogel V (2006) *Appl Environ Microbiol* 72:3005
180. Nilsson LM, Thomas WE, Trintchina E, Vogel V, Sokurenko EV (2006) *J Biol Chem* 281:16656
181. Thomas W, Forero M, Yakovenko O, Nilsson L, Vicini P, Sokurenko E, Vogel V (2006) *Biophys J* 90:753
182. Thomas WE, Nilsson LM, Forero M, Sokurenko EV, Vogel V (2004) *Mol Microbiol* 53:1545
183. Zhu C, McEver RP (2005) *Mol Cell Biomech* 2:91
184. Lou J, Zhu C (2007) *Biophys J* 92:1471
185. Hessel L, Debois H, Fletcher M, Dumas R (1999) *Eur J Clin Microbiol Infect Dis* 18:609
186. Svennerholm AM, Steele D (2004) *Best Pract Res Clin Gastroenterol* 18:421
187. Dosogne H, Vangroenweghe F, Burvenich C (2002) *Vet Res* 33:1
188. Black S, Shinefield H, Fireman B, Lewis E, Ray P, Hansen JR, Elvin L, Ensor KM, Hackell J, Siber G, Malinoski F, Madore D, Chang I, Kohberger R, Watson W, Austrian R, Edwards K (2000) *Pediatr Infect Dis J* 19:187
189. Cochi SL, O'Mara D, Preblud SR (1988) *Pediatrics* 81:166
190. Ramsay ME, Andrews N, Kaczmarski EB, Miller E (2001) *Lancet* 357:195
191. Wizemann TM, Adamou JE, Langermann S (1999) *Emerg Infect Dis* 5:395
192. Abraham SN, Babu JP, Giampapa CS, Hasty DL, Simpson WA, Beachey EH (1985) *Infect Immun* 48:625
193. O'Hanley P, Lark D, Falkow S, Schoolnik G (1985) *J Clin Invest* 75:347
194. Bertschinger HU, Nief V, Tschape H (2000) *Vet Microbiol* 71:255
195. Langermann S, Ballou WR (2003) *Adv Exp Med Biol* 539B:635
196. Stapleton A (2004) *J Urol* 171:1686
197. Morein B, Hu KF, Abusugra I (2004) *Adv Drug Deliv Rev* 56:1367
198. Schembri MA, Hasman H, Klemm P (2000) *FEMS Microbiol Lett* 188:147
199. Sung MA, Fleming K, Chen HA, Matthews S (2001) *EMBO Rep* 2:621

200. Merckel MC, Tanskanen J, Edelman S, Westerlund-Wikstrom B, Korhonen TK, Goldman A (2003) *J Mol Biol* 331:897
201. Morein B, Hu K (2001) In: Ellis RW (ed) New vaccine technologies. Landes Bioscience TX, USA p 274
202. Morein B, Lövgren-Bengtsson KL (1999) *Methods* 1:94
203. Berg V, Sellstedt M, Hedenstrom M, Pinkner JS, Hultgren SJ, Almqvist F (2006) *Bioorg Med Chem* 14:7563
204. Larsson A, Johansson SM, Pinkner JS, Hultgren SJ, Almqvist F, Kihlberg J, Linusson A (2005) *J Med Chem* 48:935
205. Pinkner JS, Remaut H, Buelens F, Miller E, Aberg V, Pemberton N, Hedenstrom M, Larsson A, Seed P, Waksman G, Hultgren SJ, Almqvist F (2006) *Proc Natl Acad Sci USA* 103:17897
206. Ofek I, Hasty DL, Sharon N (2003) *FEMS Immunol Med Microbiol* 38:181
207. Firon N, Ashkenazi S, Mirelman D, Ofek I, Sharon N (1987) *Infect Immun* 55:472
208. Zafriri D, Ofek I, Adar R, Pocino M, Sharon N (1989) *Antimicrob Agents Chemother* 33:92
209. Avorn J, Monane M, Gurwitz JH, Glynn RJ, Choodnovskiy I, Lipsitz LA (1994) *JAMA* 271:751
210. Di Martino P, Agniel R, David K, Templer C, Gaillard JL, Denys P, Botto H (2006) *World J Urol* 24:21
211. Kontiokari T, Sundqvist K, Nuutinen M, Pokka T, Koskela M, Uhari M (2001) *BMJ* 322:1571
212. Nagahori N, Lee RT, Nishimura S, Page D, Roy R, Lee YC (2002) *Chembiochem* 3:836
213. Dubber M, Sperling O, Lindhorst TK (2006) *Org Biomol Chem* 4:3901
214. Patel A, Lindhorst TK (2006) *Carbohydr Res* 341:1657
215. Mysorekar IU, Hultgren SJ (2006) *Proc Natl Acad Sci USA* 103:14170